

Identification of Products of Tetrapyrrole Pathway

Master Thesis

University of South Bohemia - Faculty of Science

Johannes Kepler University of Linz - Faculty of Engineering and
Natural Sciences

Author: Jan Hájek

Supervisor: Prof. RNDr. Josef Komenda, CSc.

Třeboň 2013

Hájek, J., 2013: Identification of Products of Tetrapyrrole Pathway. Mgr. Thesis, in English. – 60 p., Faculty of Science, University of South Bohemia, České Budějovice, Czech Republic.

I hereby declare that I have worked on my diploma thesis independently and used only the sources listed in the bibliography.

I hereby declare that, in accordance with Article 47b of Act No. 111/1998 in the valid wording, I agree with the publication of my master thesis in full form to be kept in the Faculty of Science archive, in electronic form in publicly accessible part of the STAG database operated by the University of South Bohemia in České Budějovice accessible through its web pages. Further, I agree to the electronic publication of the comments of my supervisor and thesis opponents and the record of the proceedings and results of the thesis defence in accordance with aforementioned Act No. 111/1998. I also agree to the comparison of the text of my thesis with the Theses.cz thesis database operated by the National Registry of University Theses and a plagiarism detection system.

I warrant that the thesis is my original work and that I have not received outside assistance. Only the sources cited have been used in this draft. Parts that are direct quotes or paraphrases are identified as such.

Třebon 22.4.2013

Jan Hájek

First of all, I would like to thank my Master's Thesis advisors Prof. RNDr. Josef Komenda, CSc. and Ing. Roman Sobotka, PhD. for their support and guidance.

I am especially grateful to my colleague Mgr. Pavel Hrouzek for a big help with MS Experiments in Trebon, Petr Halada, PhD for help with MS measurements and Marek Kuzma, MSc for measuring NMR Spectrum in the Laboratory of Molecular Structure Characterization of Institute of Microbiology, ASCR and Univ.-Prof. Mag. Dr. Norbert Müller for consultation of NMR results.

Content

Abstract	6
1. Introduction.....	7
1.1. Morphology of <i>Synechocystis</i>	7
1.2. Metabolism.....	9
1.2.1. Photoautotrophic grown	9
1.2.1.1. Photosynthesis of <i>Synechocystis</i>	10
1.2.1.2. Respiration of cyanobacteria	11
1.2.1.3. Tetrapyrrole pigments.....	12
1.2.1.3.1. Biosynthesis of Chlorophyll <i>a</i>	14
1.2.1.3.1.1. Reaction converting glutamic acid to protoporphyrin IX.....	14
1.2.1.3.1.2. Reaction converting protoporphyrin IX to chlorophyll	16
1.2.1.3.2. Degradation of chlorophyll.....	17
1.2.2. Heterotrophic grown.....	19
2. Aim.....	21
2.1. Material and Methods.....	22
2.1.1. Cyanobacterial strains, their cultivation and treatment	22
2.1.2. Absorption spectroscopy.....	22
2.1.3. SPE chromatography	23
2.1.4. HPLC chromatography.....	23
2.1.4.1. HILIC chromatography.....	23
2.1.4.2. C30 chromatography.....	24
2.1.5. Mass spectroscopy	24
2.1.6. Nuclear magnetic resonance	25
2.1.6.1. Nuclear magnetic resonance (Linz equipment)	25
2.1.6.2. Nuclear magnetic resonance (Prague equipment)	25
3. Results	26
3.1. Collection and spectroscopic characterization of <i>Synechocystis</i> culture supernatant	26
3.2. Concentration of the supernatant and its crude purification by methanol precipitation and solid phase extraction	28
3.3. Purification of the compounds by reverse phase C30 HPLC	31
3.4. Purification of the 414 nm compound by zic-HILIC HPLC column.....	36
3.5. NMR Results	39
3.5.1. ¹ H NMR Spectrum.....	39
3.5.2. ¹³ C NMR Spectrum.....	40

3.5.3.	COSY Spectrum	41
3.5.4.	HSQC Spectrum	42
3.5.5.	HMBC (H-C) Spectrum	43
3.5.6.	HMBC (H-N) Spectrum.....	44
3.6.	Effect of TES buffer on the formation of the 414 nm in the cell-free medium.....	45
4.	Discussion:	46
5.	Conclusions.....	51
6.	Abbreviation	52
7.	Acknowledgment.....	53
8.	Literature.....	54
9.	Attachments	58
9.1.	MALDI-TOF MS Spectrum of unpurified 414 nm compound	58
9.2.	¹ H NMR Spectrum of 9 th minute fraction from C30-HPLC.....	60

Abstract

Cultivation of a model cyanobacterium *Synechocystis* PCC 6803 under low light conditions in the presence of glucose and TES buffer leads to a change of the medium color from colorless to yellow. The absorption spectrum of the excreted unknown compound indicated a possible relationship to plant chlorophyll degradation products. To confirm this speculation the compound was purified by a combination of solid phase extraction and HPLC. The mass and NMR characteristics excluded its close relationship to modified tetrapyrroles, nevertheless the precise structure could not be determined by these means due to a complicated nature of the compound and its high polarity.

Keywords: low light cultivation, TES buffer, tetrapyrrole pathway

1. Introduction

Cyanobacteria are considered as a phylum of Gram-negative bacteria and can be found in almost every terrestrial and aquatic habitat. They are subdivided into order Chroococcales (containing e.g. *Microcystis* or *Synechocystis*), order Gloeobacterales (*Gloeobacter*), order Nostocales (e.g. *Nostoc* or *Scytonematopsis*), order Oscillatoriales, Pleurocapsales and Stigonematales. Cyanobacteria are thought to be among the evolutionarily oldest organisms, 3.5 billion years microfossils are classified to be cyanobacteria¹. The main reason for evolutionary hardiness of cyanobacteria is their ability to grow phototrophically as well as heterotrophically. Heterotrophic growth happens mostly via glycolysis followed by oxidative phosphorylation, phototrophic growth happens via oxygenic photosynthesis. Cyanobacteria possess two photosystems that are similar to those found in plants. Some cyanobacteria are also able to fix nitrogen and this makes them independent on nitrate or ammonium ions.

Synechocystis sp. PCC 6803 belongs to the most frequently studied species of cyanobacteria and has become nowadays a model organism. The strain was originally isolated from fresh water lake² and was deposited in the Pasteur Culture Collection in 1968. This species is able to survive and grow under a wide range of conditions. If suitable carbon source is provided, *Synechocystis* sp. PCC 6803 can grow in the absence of photosynthesis. Its genome consists of one chromosome (size 3.57 megabases), three small plasmids (5.2, 2.4, and 2.3 kilobases) and four large plasmids (120, 106, 103, and 44 kilobases). All these DNA molecules are always present in several copies (up to ten copies per cell)³.

1.1. Morphology of *Synechocystis*

Synechocystis as a member of Chroococcales occurs in the form of single floating spherical cells with a diameter of 1-5 micrometers⁴, which frequently form a pair due to their frequent binary fission typical for bacteria.

Cyanobacteria including *Synechocystis* are considered as Gram-negative bacteria and therefore they possess two membranes on the cellular surface. As they are prokaryotes in contrast to eukaryotic microalgae they contain no typical sub-cellular organelles. The cyanobacterial outer membrane slightly differs from typical Gram-negative bacteria outer membrane as it contains a small amount of bound phosphate that is not typical for Gram-negative bacteria and often lacks ketodeoxyoctonate – a common lipopolysaccharide of Gram-negative bacteria outer membrane⁵.

There are also differences between cyanobacteria and typical Gram-negative bacteria in the properties of peptidoglycan layer, the only solid part of the cyanobacterial cell. This layer is much thicker in cyanobacteria than in most Gram-negative bacteria, its thickness varies from 10 nm up to 700 nm⁵. There is also a difference in the level of peptidoglycan crosslinking. The usual degree of crosslinking found in Gram-negative bacteria is about 20-33%⁶, but degree of cross-linking in *Synechocystis* strains can reach up to 63%⁷. This level of crosslinking is more typical for Gram-positive bacteria. On the other hand, the cyanobacterial pentapeptides, which cross-link the peptidoglycan, contain only the typical gram-negative bacterial compound acid *meso*-diaminopimelic acid, while L-diaminopimelic acid or L-lysine are constituents of tetrapeptides in the Gram-positive peptidoglycan⁸.

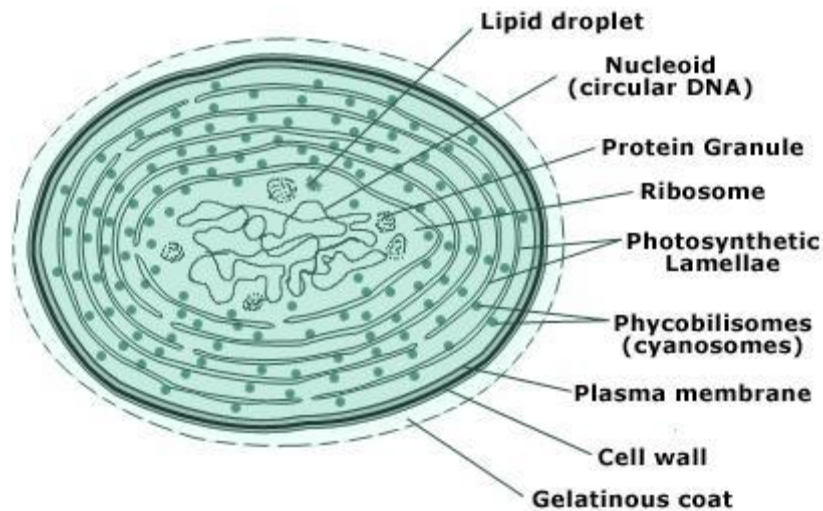


Figure 1: Structure of cyanobacterial cell ⁹

1.2. Metabolism

1.2.1. Photoautotrophic grown

Under photoautotrophic condition, cyanobacteria uses light energy absorbed by various pigments for formation of ATP and NADPH needed for assimilation of CO₂ and for many other various biosynthetic reactions and processes in the cell. As ubiquitous oxygenic phototrophic bacteria, cyanobacteria are carrying out in the same noncompartmentalized prokaryotic cell on the one hand water-splitting, O₂-releasing photosynthesis and on the other hand water-forming and O₂-reducing respiration. These processes require the strict separate regulation of both processes which might be facilitated by the existence of separate membrane compartments. There are two types of morphologically more or less separate bioenergetically active membrane systems in cyanobacteria. Intracytoplasmatic thylakoid membranes containing chlorophyll are capable of both photosynthetic and respiratory

The energy from phycobilisomes is transferred to the reaction center of PSII which performs charge separation¹³. The oxidized form of the PSII primary donor P680 withdraws electrons from water via oxygen evolving complex. This metallo-oxo cluster consists of four manganese and one calcium ions which are bridged by oxygen atoms and bind water molecules¹⁴. The withdrawn electrons reduce the plastoquinone (PQ) pool via a system of PSII electron acceptors - pheophytin and two plastoquinone molecules Q_A and Q_B. PQ pool reduces the cytochrome b₆f complex and electrons are further transferred to luminal redox active polypeptides cytochrome c₅₅₃ or plastocyanin. These electron carriers reduce the oxidized primary donor P700 of the Photosystem I (PSI) reaction center. The electron acceptors of PSI transfer electrons via ferredoxin to NADP that could be further used for CO₂ assimilation¹⁵. Components involved in the transfer of electron on the acceptor side PSII are chlorophyll monomer A0, phylloquinone and three 4Fe-4S iron-sulphur clusters (Fx, Fa and Fb)¹⁶. The photosynthetic electron flow from water to NADP leads to the vectorial transport of protons across the photosynthetic membrane and resulting pH gradient is used for ATP synthesis by ATP synthase.

1.2.1.2. Respiration of cyanobacteria

As mentioned above, cyanobacteria may contain two independent respiratory chains – one located in cytoplasmic membrane, the other one in thylakoids - although the electron transport chain of the cytoplasmic membrane is not yet well characterized in any strain. Respiration in thylakoids could be divided into three different functional parts – the one connected with NAD(P)H oxidation, the one connected with succinate dehydrogenase and the one involving terminal oxidases.

Oxidation of NAD(P)H is performed by an enzyme NADH dehydrogenase (NDH) complex similar to the 14-subunit NDH-1 complex from *Escherichia coli*, except that three

subunits involved with substrate binding are not apparent from the cyanobacterial genome and creates respiratory electron flow into the PQ pool. Minor part of respiration could be proceed on type-2 NDH which is a single-subunit protein and that may not contribute to a proton gradient over the thylakoid membrane¹⁷.

Succinate dehydrogenase (SDH) is the second potentially respiratory electron donor to the PQ pool. Succinate dehydrogenase has a major effect on the PQ redox poise, mutants lacking this enzyme showed a much more oxidized PQ pool than the wild type strains¹⁸.

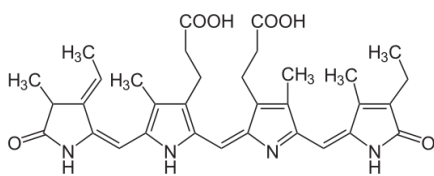
Finally, there are three types of thylakoid-localized terminal respiratory oxidases aa₃-type cytochrome c oxidase, cytochrome bd-quinol oxidase and the alternative respiratory terminal oxidase. All of these play an important role in the efficient dark respiration, reduction of oxidative stress and accommodation of sudden light changes, demonstrating the strong selective pressure to maintain linked photosynthetic and respiratory electron chains within the thylakoid membrane¹⁹.

1.2.1.3. Tetrapyrrole pigments

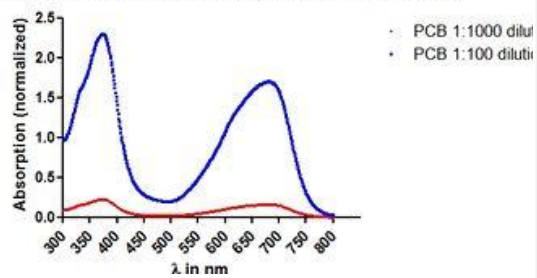
As already mentioned, the efficient electron transport flow is driven by energy which must be captured by a large number of pigments. The main peripheral pigments of cyanobacteria are linear tetrapyrroles. Overview of their structures and absorption properties is shown in Fig. 3a^{20,21,22,23}. Nevertheless, the most important cyanobacterial photosynthetic pigment is the cyclic tetrapyrrole chlorophyll *a* that absorbs energy in visible light region except green light (500-600 nm). Structure and absorption spectrum of chlorophyll *a* is shown in Fig. 3b²⁴.

Linear tetrapyrrole

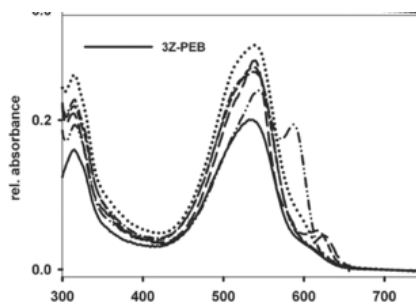
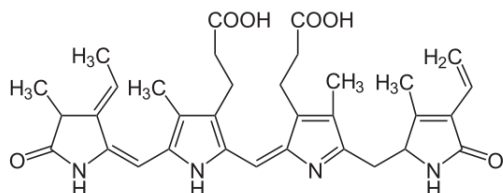
a)



Absorption spectrum of extracted phycocyanobilin (PCB)



b)



c)

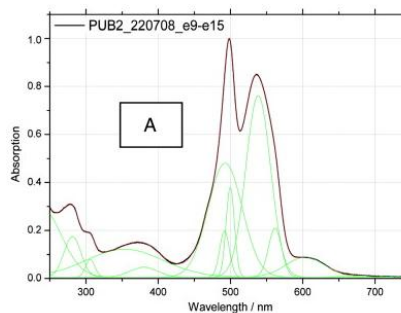
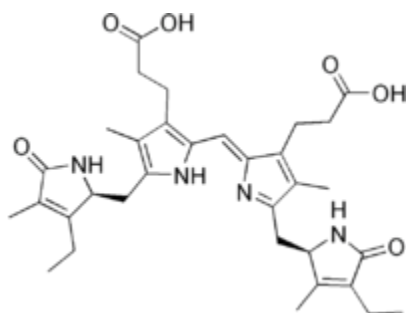


Figure 3a: Overview of structures and absorption spectra of linear tetrapyrrole pigments involved in absorbing light and utilization of its energy for driving the photosynthetic electron transport chains. a) phycocyanobilin b) phycoerythrobilin c) phycoerythrin^{20,21,22,23}

Chlorophyll *a*

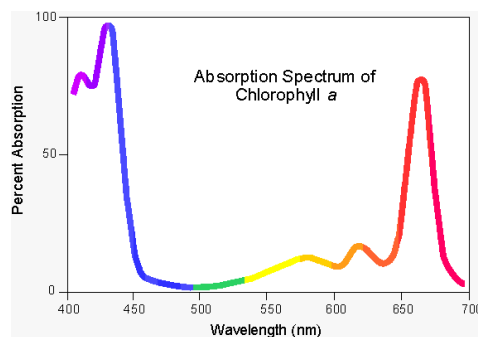
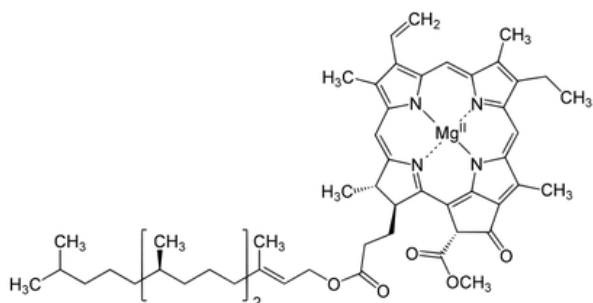


Figure 3b: Structure and absorption spectrum of Chlorophyll *a*²⁴

1.2.1.3.1. Biosynthesis of Chlorophyll *a*

Biosynthesis of chlorophyll *a* could be splitted into two series of reactions. In the first one glutamic acid, usually synthesized from oxo-glutaric acid of the citric acid cycle, is converted into δ -aminolevulinic acid and further to protoporphyrin IX. These reactions are common for most of tetrapyrroles including heme or chlorophyll. The second series of reactions is specific, protoporphyrin IX is converted firstly into chlorophyllide and finally to chlorophyll *a*.

1.2.1.3.1.1. Reaction converting glutamic acid to protoporphyrin IX

Biosynthesis of chlorophyll starts with glutamic acid that is activated with ATP and reacts with t-RNA. The newly formed glutamyl-tRNA is reduced to glutamate-1-semialdehyde NADPH is used as cofactor for this reaction. Glutamate-1-semialdehyde is shortened by one carbon to produce δ -aminolevulinic acid as crucial intermediate in the tetrapyrrole biosynthetic pathway. Condensation of two molecules of δ -aminolevulinic acid leads to formation of derivative of pyrrole – porphobilinogen – as a basic unit of chlorophyll. Porphobilinogen easily polymerizes and forms linear tetrapyrrole hydroxymethylbilane. Dehydration of hydroxymethylbilane creates afterwards cyclic porphyrin uroporphyrinogen III. This compound contains 8 carboxylic groups. Firstly four of them are cleaved off to produce coproporphyrinogen III, subsequently two more carboxyls are removed to form protoporphyrinogen IX. Finally protoporphyrin IX is created by reduction of two pyrrole-subunits of protoporphyrinogen IX²⁵. The whole scheme of these reactions is shown on Fig. 4.

Biosynthesis of chlorophyll – glutamic acid to protoporphyrin IX

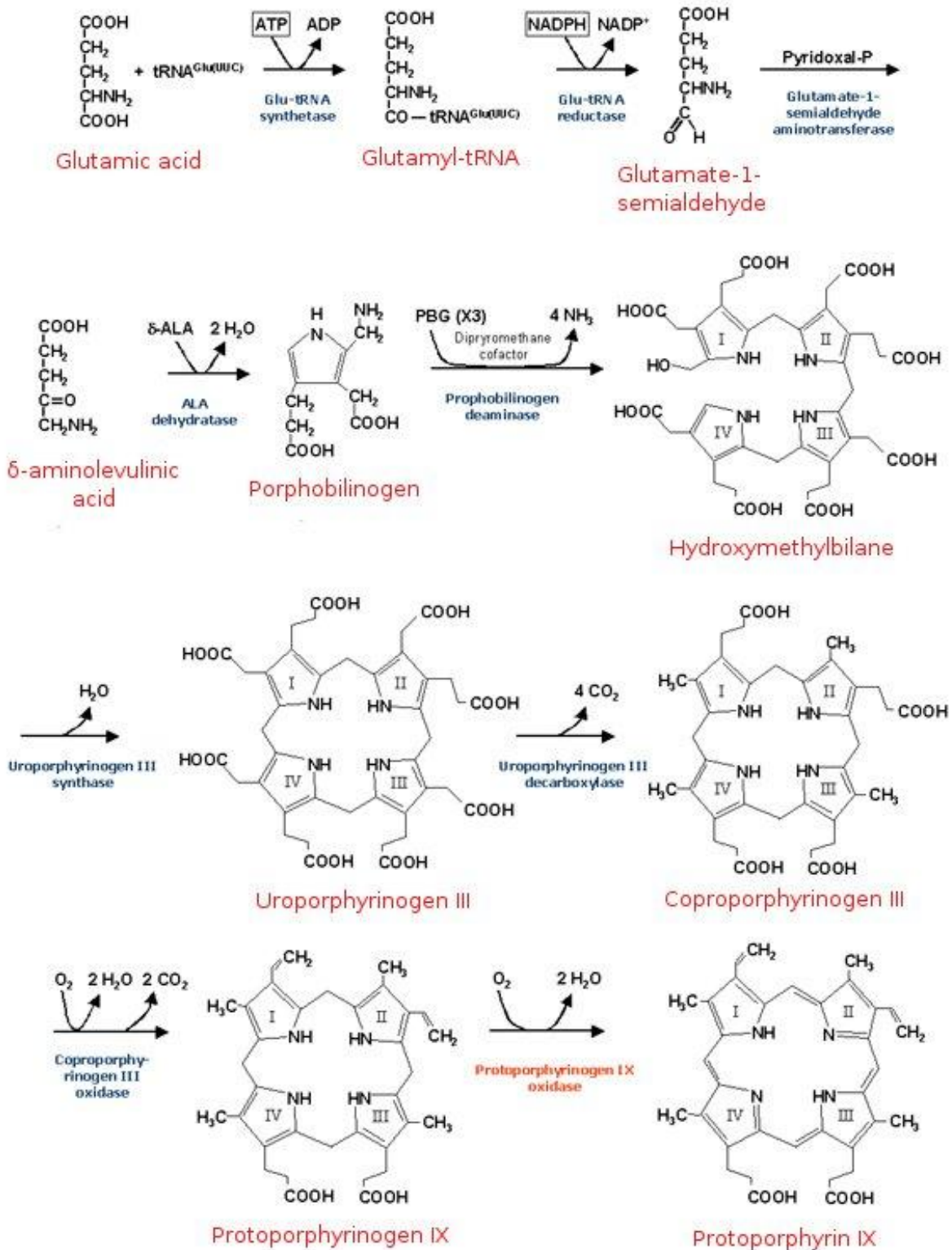


Figure 4: Overview of reactions of biosynthesis of protoporphyrin IX, precursor of chlorophyll *a*, from glutamic acid²⁵

1.2.1.3.1.2. Reaction converting protoporphyrin IX to chlorophyll

In the first part of the chlorophyll-specific tetrapyrrole biosynthetic branch, Mg^{2+} ion is incorporated into protoporphyrin IX, one carboxyl is methylated, isocyclic ring is formed and one vinyl is reduced yielding monovinyl protochlorophyllide. This molecule is reduced to chlorophyllide in an unique photoreaction which requires not only NADPH but also at least one photon. The reaction is catalyzed by light-dependent protochlorophyllide oxidoreductase

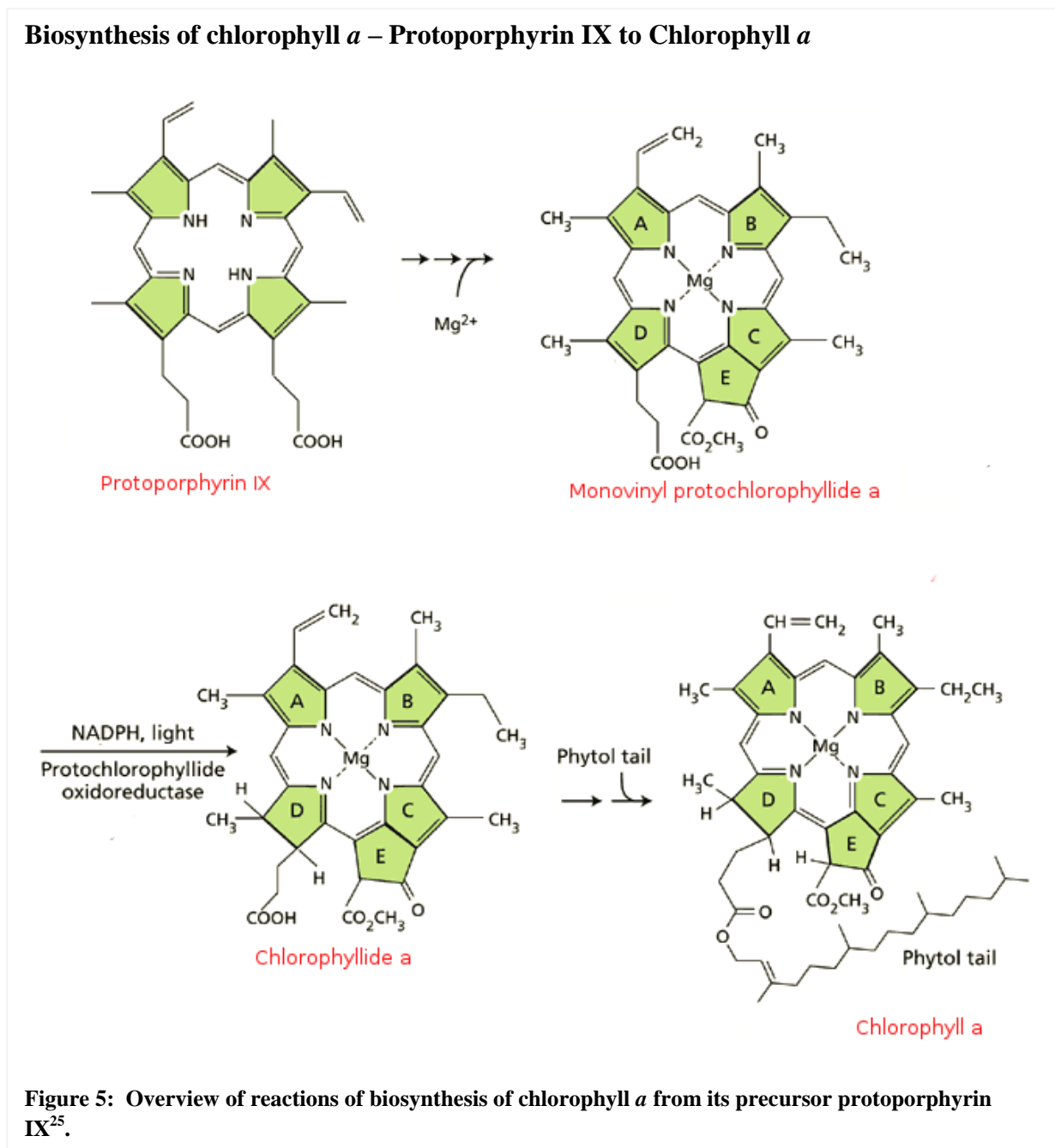


Figure 5: Overview of reactions of biosynthesis of chlorophyll *a* from its precursor protoporphyrin IX²⁵.

(POR) although cyanobacteria may alternatively reduce protochlorophyllide in the dark using dark-operative POR. Chlorophyll *a* biosynthesis is finished by addition of acyclic diterpene termed phytol. The simplified scheme of chlorophyll-specific biosynthetic reactions is shown in Fig. 5²⁵.

1.2.1.3.2. Degradation of chlorophyll

The catabolism of chlorophyll in cyanobacteria is not characterized yet, most studies were performed only in plants. The plant catabolic machinery comprises at least six known reactions²⁶. At the very beginning, chlorophyll *a* is dephytylated to chlorophyllide *a* and then Mg^{2+} ion is removed. The product of this reaction – pheophorbide *a* – is the last colored (green) catabolite of chlorophyll degradation pathway. The porphyrin ring of pheophorbide *a* is oxygenolytically opened forming red chlorophyll catabolite (RCC) and then reduced to primary fluorescent chlorophyll catabolite (pFCC). Further reduction leads to final non-fluorescent chlorophyll catabolites (NCCs) that are excreted to vacuoles. The degradation pathway is shown in Fig. 6, spectra of degradation products are summarized in Fig. 7²⁷.

Degradation of chlorophyll

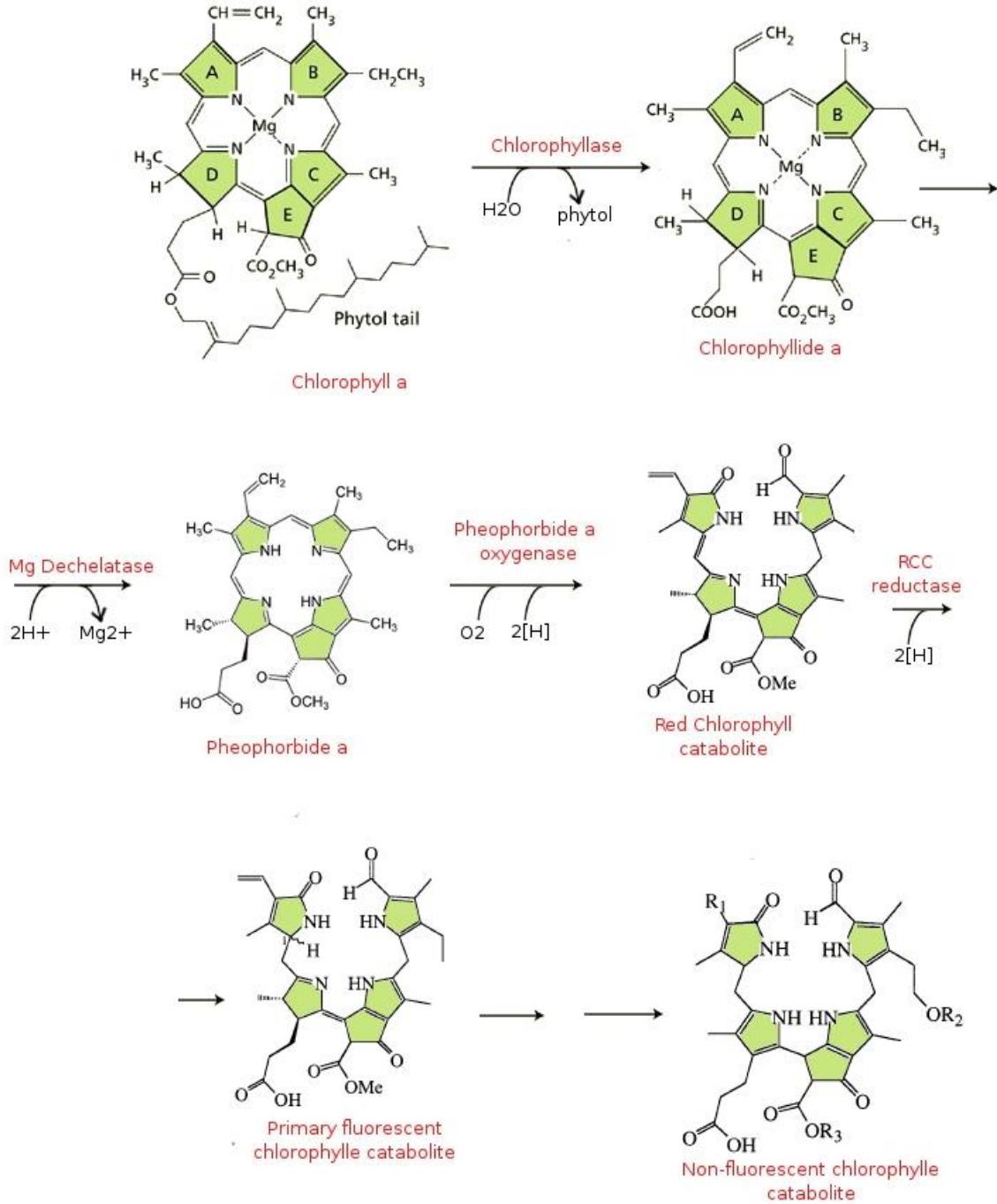


Figure 6: Catabolism of chlorophyll a²⁶

Absorption spectra of chlorophyll catabolism

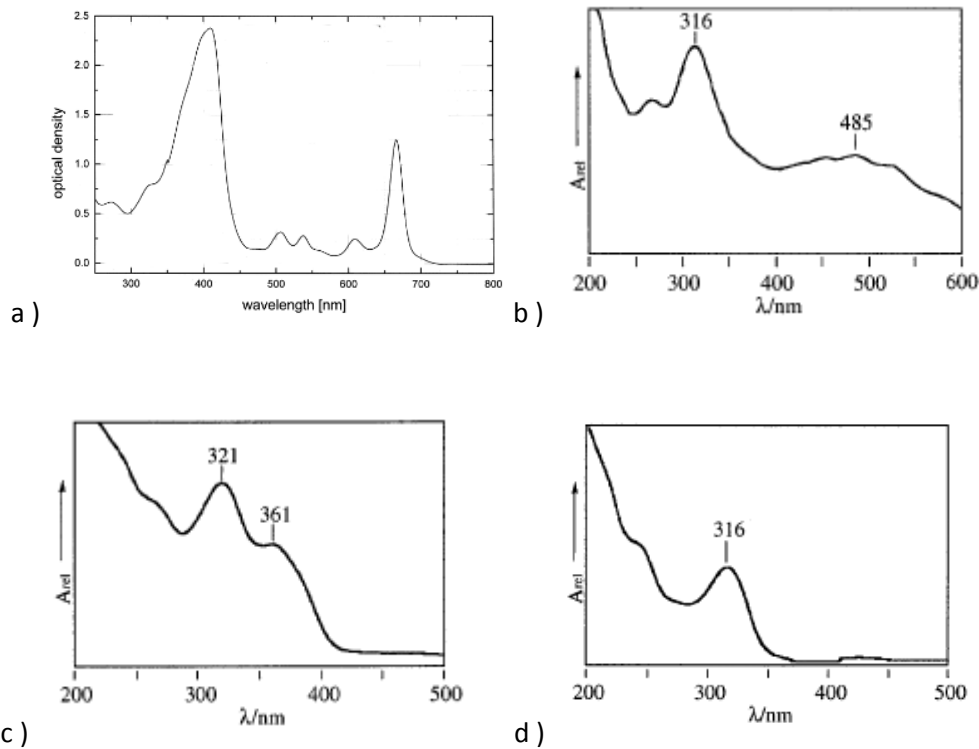


Figure 7: Absorption spectra of chlorophyll catabolites a) Absorption spectrum of pheophorbide *a*; b) Absorption spectrum of red chlorophyll catabolite; c) Absorption spectrum of primary fluorescent chlorophyll catabolite; d) Absorption spectrum of non-fluorescent chlorophyll catabolites²⁷

1.2.2. Heterotrophic grown

Some cyanobacteria are capable of growth not only in the light using CO_2 as carbon source but also under conditions where growth is dependent on exogenous organic compounds. Such heterotrophic growth can occur in the light (photoheterotrophy) or in the complete darkness (chemoheterotrophy). In the second case, only the organic compound (such as glucose) provides the organism a source of carbon and energy. That means that heterotrophic growth is totally dependent on exogenous organic compound in medium. Organic compounds are under these circumstances metabolized via oxidative pentose-

phosphate cycle as shown on Fig. 8²⁸.

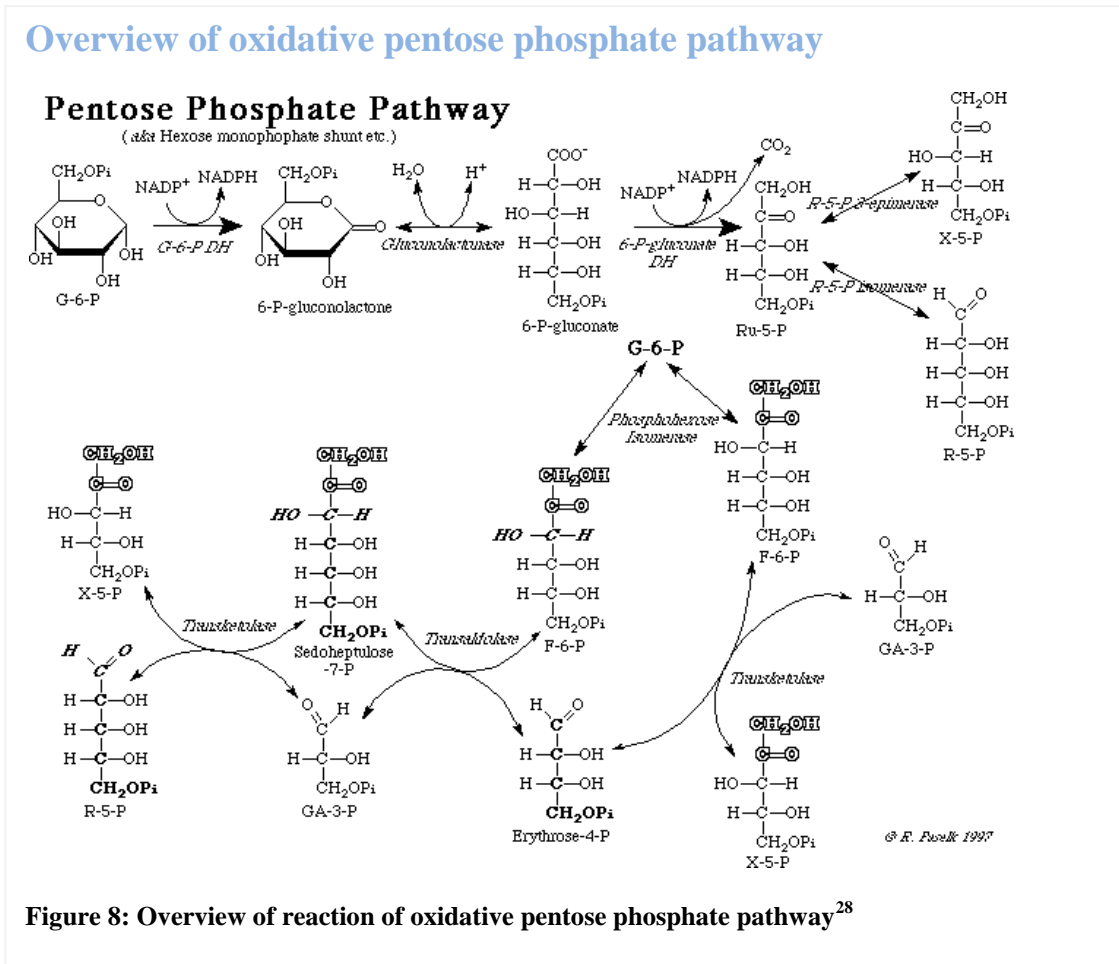


Figure 8: Overview of reaction of oxidative pentose phosphate pathway²⁸

2. Aim

Synechocystis sp. PCC 6803, the cyanobacterial species used in this study, is a phototrophic microorganism but upon addition of glucose to the growth medium (usually used concentration is 5 mM) it also grows photoheterotrophically. Interestingly, when grown in the presence of glucose under low light conditions (LL, 5 $\mu\text{mol photons m}^{-2} \text{ s}^{-1}$), the cells excrete into the medium unknown substances causing dark reddish coloration of the medium which becomes apparent after sedimenting the cells by centrifugation. Moreover, when the medium also contains biological buffer TES (2-[[1,3-dihydroxy-2-(hydroxymethyl)propan-2-yl]amino]ethanesulfonic acid) for stabilization of pH during growth, the medium changes color to yellow. In contrast, under normal light conditions (NL, 40 $\mu\text{mol photons m}^{-2} \text{ s}^{-1}$) even in the presence of glucose and TES, the cultivation medium remains colorless indicating either light sensitivity of excreted substances, or absence of their accumulation under higher irradiance. Preliminary data showed that the excreted substances exhibit absorption spectra with maxima around 360 and 320 nm, in the presence of TES the additional peak at about 416 nm is also formed. Since similar spectra are typical for certain degradation products of chlorophyll in plants (Fig. 7) and coloration of the medium is faster in mutants with defects in synthesis of chlorophyll-proteins (for instance mutant lacking Photosystem I²⁹), it has been speculated that the excreted substances are related to the metabolism of chlorophyll.

The aim of the thesis was to purify, characterize and determine the structure and origin of the yellow compound excreted by *Synechocystis* cells into the growth medium under specific conditions.

2.1. Material and Methods

2.1.1. Cyanobacterial strains, their cultivation and treatment

If not stated otherwise the glucose tolerant wild type (WT) strain of *Synechocystis* PCC 6803 was grown in liquid BG-11 medium³⁰ (composition see Table 1) containing 5 mM glucose with or without 10 mM TES buffer at 30°C and 5 $\mu\text{mol photons m}^{-2} \text{s}^{-1}$ (low light, LL) on the rotary shaker. To get substances excreted into the medium, the culture was centrifuged at 8 000 rpm (5 000 x g) for 10 min in the Sigma centrifuge. The sedimented cells were discarded and the supernatant was used as the source of excreted substances for further study.

Table 1: Composition and preparation of BG-11

BG11		Trace metal mix	
NaNO ₃	1.5 g	H ₃ BO ₃	2.86 g
K ₂ HPO ₄	0.04 g	MnCl ₂ ·4H ₂ O	1.81 g
MgSO ₄ ·7H ₂ O	0.075 g	ZnSO ₄ ·7H ₂ O	0.222 g
CaCl ₂ ·2H ₂ O	0.036 g	NaMoO ₄ ·2H ₂ O	0.39 g
Citric acid	0.006 g	CuSO ₄ ·5H ₂ O	0.079 g
Ferric ammonium citrate	0.006 g	Co(NO ₃) ₂ ·6H ₂ O	49.4 mg
EDTA (disodium salt)	0.001 g	Distilled water	1.0 L
NaCO ₃	0.02 g		
Trace metal mix A5	1.0 ml		
distilled water	1 l		

2.1.2. Absorption spectroscopy

Absorption spectra of cell cultures and supernatants after centrifugation the cell were measured using Shimadzu UV3000 Dual-Wavelength Double-Beam Spectrophotometer.

2.1.3. SPE chromatography

For solid phase extraction CHROMABOND[®] NH₂ cartridge (SPE NH₂-cartridge, pore size 60 Å, particle size 45 µm, specific surface 500 m²/g, pH stability 2–8; aminopropyl phase, carbon content 3.5 %) was used, elution was performed by solutions with different concentrations of ammonium acetate buffer. Eluate obtained using 0.5 M ammonium acetate contained compound(s) with absorption maxima at 414 nm, 360 nm and 330 nm and was collected for further experiments.

Table 2: Solvents used for SPE NH₂-cartridge.

	Solvent
Wash	0.01 M NH ₄ Ac
Elution	0.5 M NH ₄ Ac
Cleaning	4 M NH ₄ Ac

2.1.4. HPLC chromatography

HPLC-chromatographic separations of eluate components were done using Agilent 1200 Series HPLC equipped with degasser, quaternary pump, autosampler, thermostatted column compartment, Diode array detector and either two fluorescence detectors or MS-instrument.

2.1.4.1. HILIC chromatography

Hydrophilic chromatography (HILIC) was performed using solvent system containing acetonitrile and deionized water. Column SeQuant[®] ZIC[®]-HILIC (5µm, 200Å) PEEK 150 x 4.6 mm was used. Maximum injection volume per run was 50 µl, column temperature was not

controlled, fractions were manually collected. The fraction containing compound with absorption maximum at 414 nm was collected for further study.

Table 3: Timetable of solvent composition in HILIC-HPLC

Time	Solvent	flowrate	max pressure
0-20 min	100% acetonitrile => 60% acetonitrile	0.5 ml/min	300 bar
20-35 min	60% acetonitrile => 40% acetonitrile	0.6 ml/min	300 bar
35-45	Water	0.6 ml/min	300 bar

2.1.4.2. C30 chromatography

Reverse phase C30 chromatography was performed using solvent system containing ammonium acetate buffer and methanol and YMC C30 HPLC column, 5 μ m, 250 x 4.6 mm. Maximum injection per run was 100 μ l, column temperature was not controlled, all fraction were manually collected. Fraction containing compound with absorption maximum at 414 nm was collected for further study.

Table 4: Timetable of solvent composition in C30-HPLC

Time	Solvent	Flowrate	max pressure
0-11 min	100% 0.05 M NH ₄ Ac	0.6 ml/min	300 bar
11-25 min	100% 0.05 M NH ₄ Ac => 100% Methanol	0.6 ml/min	300 bar
25-46 min	100% Methanol	0.6 ml/min	300 bar

2.1.5. Mass spectroscopy

Mass spectra of purified samples were measured using Agilent MS 6300 Series Ion Trap equipped with electrospray ionization (ESI). Samples were either directly injected or prepurified with connected HPLC reverse phase C30 column. ESI setting was set following: nebulizer pressure 7.5 psi; dry gas flow 10 l/min; dry temperature 325 °C.

2.1.6. Nuclear magnetic resonance

2.1.6.1. Nuclear magnetic resonance (Linz equipment)

NMR-spectra were measured using Bruker digital Avance III NMR-spectrometer at 300 and 700 MHz. Samples were dissolved in Cl_2CD_2 . All spectra were afterwards analyzed using Bruker software TOPSPIN Version 3.0.

2.1.6.2. Nuclear magnetic resonance (Prague equipment)

NMR-spectra were measured using Bruker digital Avance III NMR-spectrometer at 700 MHz. Samples were dissolved in D_2O . All spectra were afterwards analyzed using Bruker software TOPSPIN Version 3.0, ACD/NMR Processor release 12.01 and MestReNova 8.1.1. For prediction of ^{13}C and ^1H NMR Spectrum ChemDraw Ultra 12.0 was used.

3. Results

3.1. Collection and spectroscopic characterization of *Synechocystis* culture

supernatant

The *Synechocystis* WT strain was grown under low irradiance photoheterotrophically in the presence and absence of TES and after 3 days of growth the cell suspension was centrifuged and supernatant was collected (500 ml). In the case of culture grown in the absence of TES the supernatant was reddish (Fig. 9) while the supernatant from TES-cultivated cells was yellow (Fig. 10). This difference was confirmed by UV/VIS spectroscopy (according to absorption spectrum in Fig. 11 and 12). Unlike the TES-free medium, the absorption spectrum of the TES-containing medium exhibited a new absorption maximum at about 410 nm. Other main absorption maxima at 360 nm and 330 nm were similar for both media.



Figure 10: Appearance of the cultivation medium obtained by centrifugation of *Synechocystis* WT strain culture grown in the presence of 5 mM glucose and 10 mM TES under low light conditions.



Figure 9: Appearance of the cultivation medium obtained by centrifugation of *Synechocystis* WT strain culture grown in the presence of 5 mM glucose without TES under low light conditions.

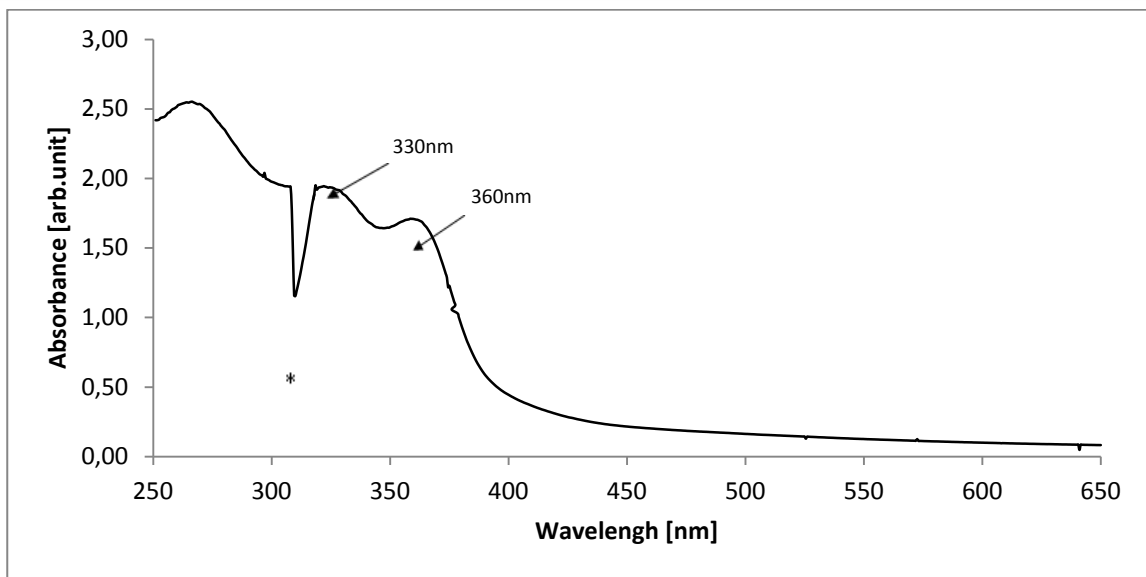


Figure 11: Absorption spectrum of the cultivation medium obtained by centrifugation of the *Synechocystis* WT strain culture grown in the presence of 5 mM glucose at low light. Asterisk indicates the artefactual spike at 310 nm caused by switch between the halogen and deuterium lamp

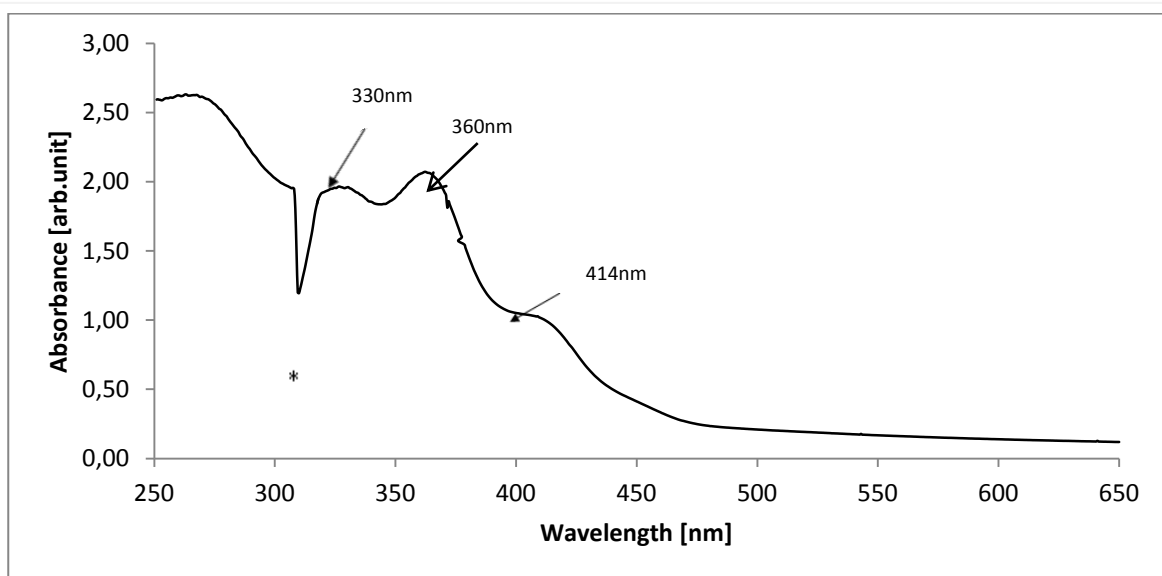


Figure 12: Absorption spectrum of the cultivation medium obtained by centrifugation of the *Synechocystis* WT strain culture grown in the presence of 5 mM glucose and 10 mM TES at low light. Asterisk indicates the artefactual spike at 310 nm caused by switch between the halogen and deuterium lamp

3.2. Concentration of the supernatant and its crude purification by methanol precipitation and solid phase extraction

At the very beginning the medium was filtrated with syringe filters (0.45 μm pores) to get rid of rests of cells. Because of the large volume (hundreds of milliliters) of the medium after centrifugation, it was necessary to reduce the overall volume before purification via evaporation. On rotary evaporator the medium was evaporated from 500 ml to about 20 ml. Temperature did not rise over 40 $^{\circ}\text{C}$. Using UV/VIS absorption spectroscopy no changes in the character of the spectra were detected after evaporation.

To get rid of unwanted compounds methanol was added (80 ml methanol per 20 ml medium). This addition caused precipitation of more than 10 mg of unknown compounds in the form of red crystals containing for instance a protein hemolysin. So, in this way an enrichment of the compound(s) of our interest and increase in its relative content was reached as indicated by Fig. 13 and 14.

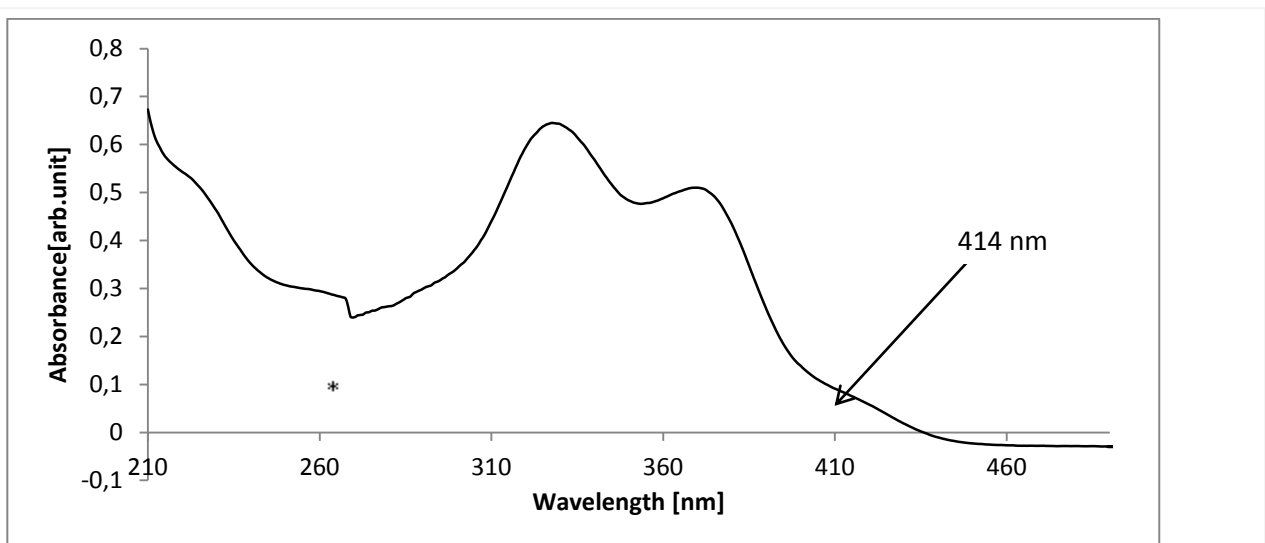


Figure 13: Absorption spectrum of the methanol insoluble fraction of medium from *Synechocystis* WT strain culture grown in the presence of 5 mM glucose and 10 mM TES at low light. Asterisk indicates the artefactual spike at 270 nm caused by switch between the halogen and deuterium lamp

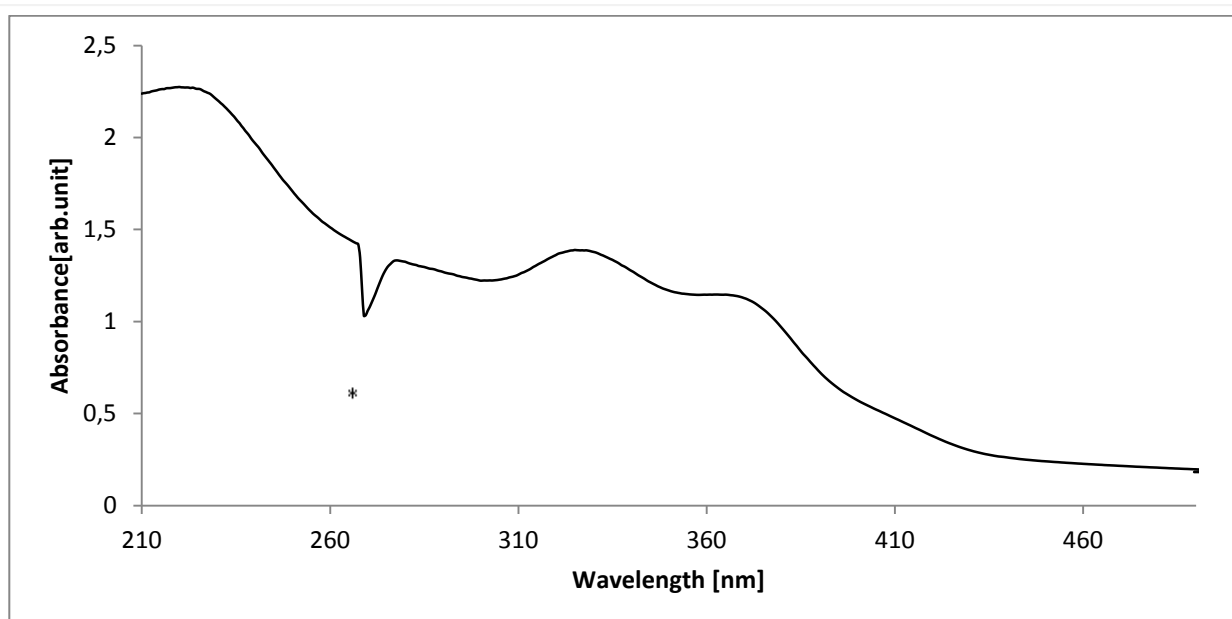


Figure 14: Absorption spectrum of methanol soluble fraction of medium from *Synechocystis* WT strain culture grown in the presence of 5 mM glucose and 10 mM TES at low light. Asterisk indicates the artefactual spike at 270nm caused by switch between the halogen and deuterium lamp

To concentrate and further purify the substance(s) with the absorption maxima in the solution at 330, 380 and 410 nm, we tested different ionex cartridges, but most of the tests were not successful. Either the compound did not bind to the cartridge at all (in case of e.g. DEAE-cellulose) or it was necessary to use high concentration of salts to elute it (in the case of tertiary amine cartridge). The only cartridges that showed a suitable strength of retention were cartridges with bound amino group (SPE NH₂ cartridge).

SPE NH₂ cartridge was firstly washed with 0.01 M ammonium acetate (about 10 volumes of the cartridge), afterwards with methanol and then again with 0.01 M ammonium acetate. To elute the substances of our interest, 0.5 M ammonium acetate was necessary to use. Finally, it was necessary to clean the cartridge with 4 M ammonium acetate to remove the red precipitate, which was bound on the top of the cartridge (this compound had similar spectrum as methanol precipitated crystals) as seen on absorption spectra on Fig. 15 and 16.

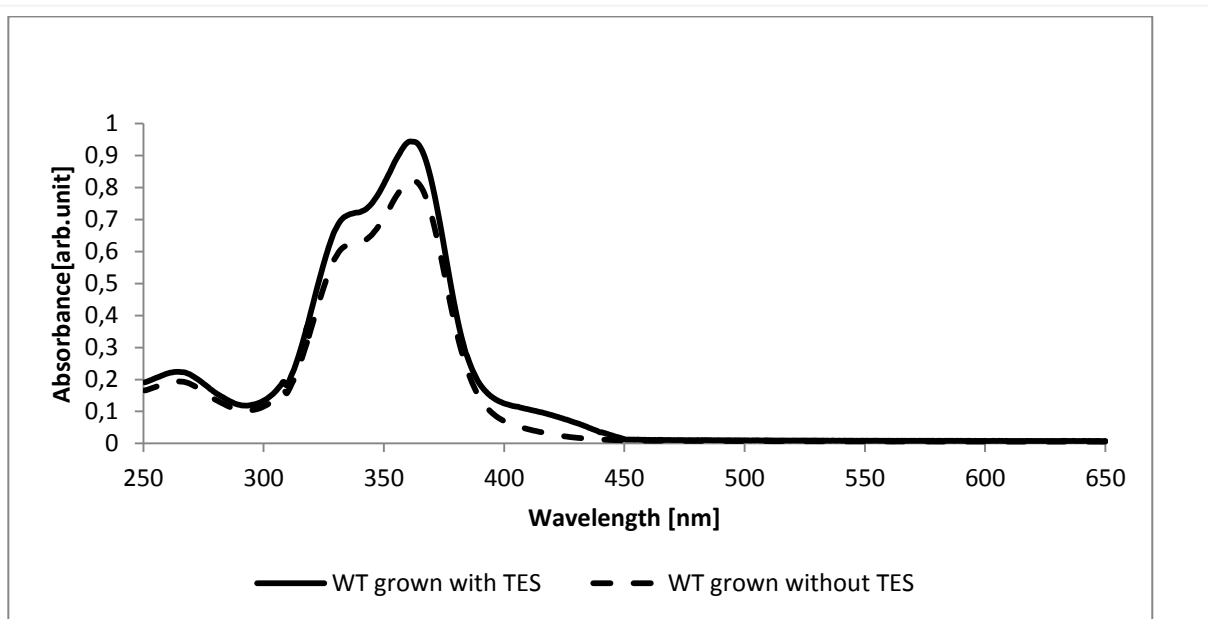


Figure 15: Absorption spectrum of fraction got by elution with 0.05 M ammonium acetate from NH₂ SPE cartridge. Continuous line – *Synechocystis* WT strain culture grown in the presence of 5 mM glucose and 10 mM TES at low light; Dashed line – *Synechocystis* WT strain culture grown in the presence of 5 mM glucose and absence of TES at low light.

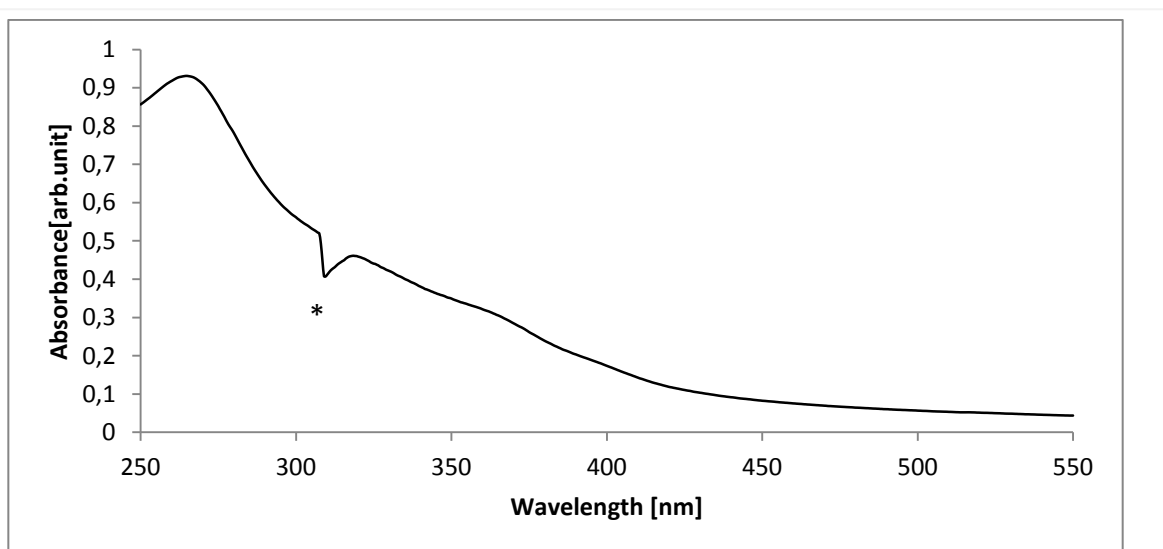


Figure 16: Absorption spectrum of fraction got by cleaning of NH₂ SPE cartridge with 4 M ammonium acetate. The identical spectrum is for *Synechocystis* WT strain culture grown in the presence of 5 mM glucose and 10 mM TES at low light. Asterisk indicates the artefactual spike at 270 nm caused by switch between the halogen and deuterium lamp

The 0.5 M ammonium acetate eluate was again concentrated by evaporation until the volume was small enough (few milliliters) to allow separation of the components using

analytical HPLC. A NH_2 -column could not be used for HPLC chromatography due to the need of high salt concentration necessary for elution, which was not compatible with the use of MS detector. Therefore we used reverse phase C30 and hydrophilic HPLC columns for further purification.

3.3. Purification of the compounds by reverse phase C30 HPLC

During C30 HPLC our maximum injection volume per run was only 100 μl (totally more than 40 runs were performed) and we monitored the separation using a diode array

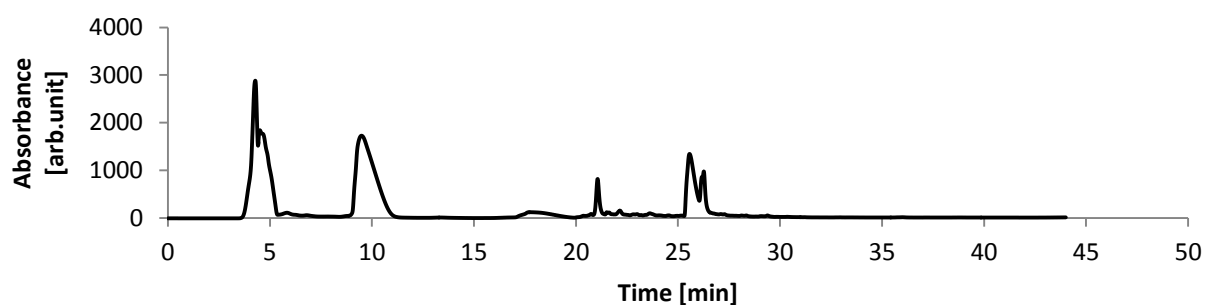


Figure 17a: C30-Chromatogram (wavelength=270 nm) of 0.5 M ammonium acetate fraction from NH_2 cartridge from *Synechocystis* WT strain culture grown in the presence of 5 mM glucose and 10 mM TES at low light

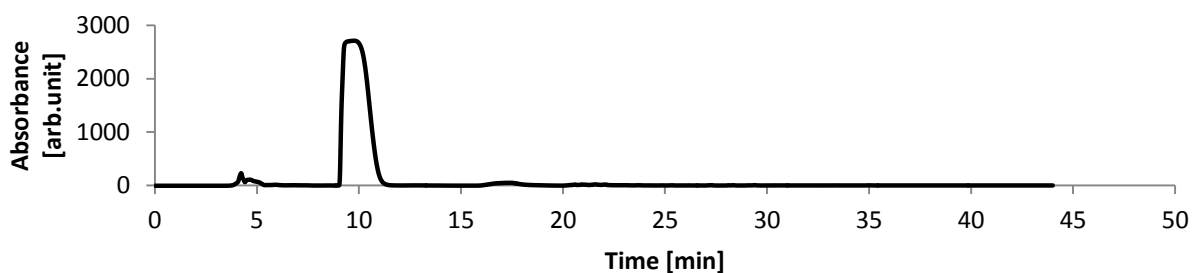


Figure 17b: C30-Chromatogram (wavelength=420 nm) of 0.5 M ammonium acetate fraction from NH_2 cartridge from *Synechocystis* WT strain culture grown in the presence of 5 mM glucose and 10 mM TES at low light

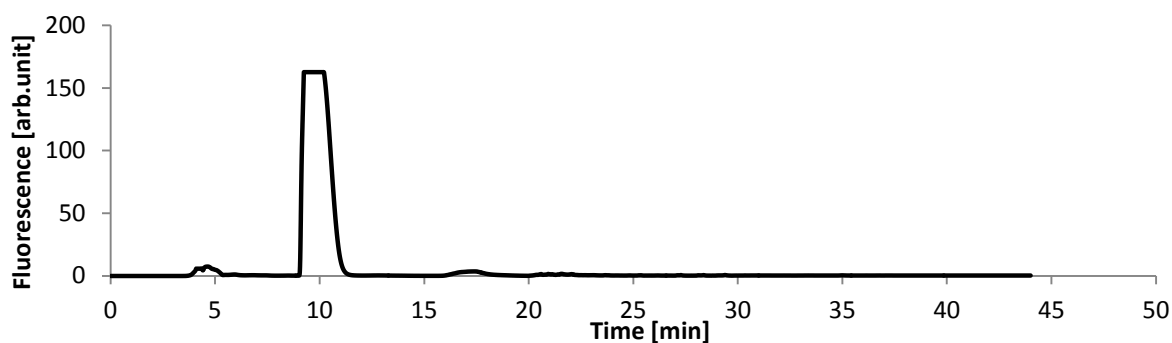


Figure 17c: C30-Chromatogram (excitation wavelength=420 nm, emission wavelength=540nm) of 0.5 M ammonium acetate fraction from NH_2 cartridge from *Synechocystis* WT strain culture grown in the presence of 5 mM glucose and 10 mM TES at low light

detector with set wavelength at 420 nm and using fluorescence detector with the same excitation wavelength. Chromatograms are shown in Fig. 17a, b and c.

Using the C30 column, the substance with 330-360 nm maximum (Fig. 18) eluted from the column shortly after the injection peak at elution time about 3rd min. The compound with peak at 414 nm eluted using 0.05 M ammonium acetate at about 9th min (Fig. 19).

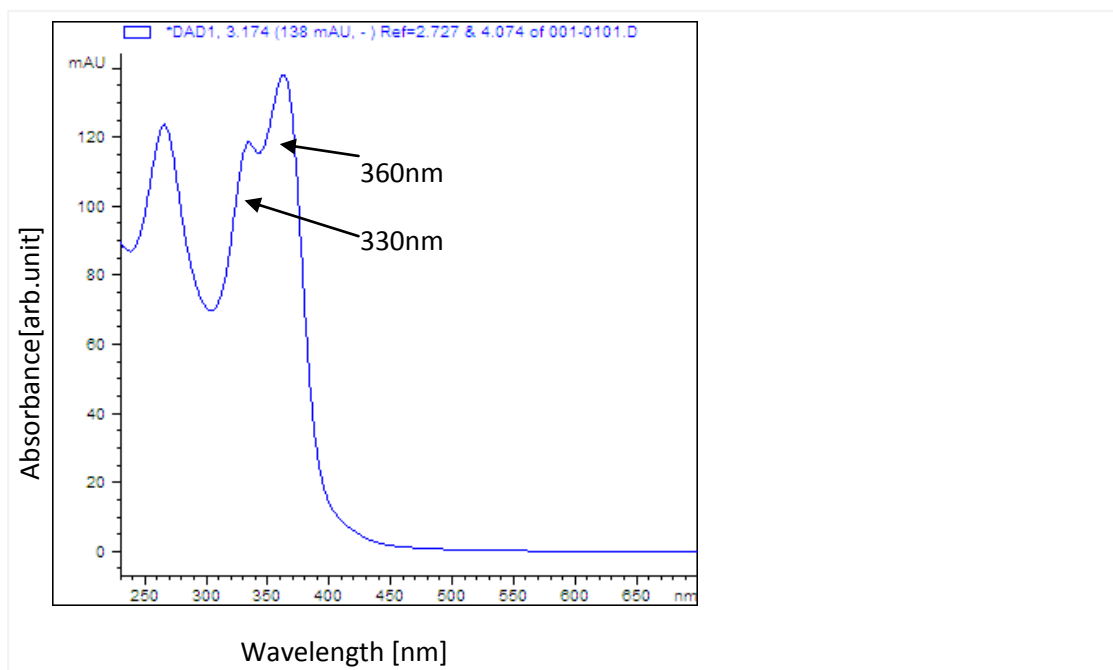


Figure 18: Absorption spectrum of peak at 3.2 min of C30-HPLC chromatogram
(*Synechocystis* WT strain culture grown in the presence of 5 mM glucose and 10 mM TES under low light conditions)

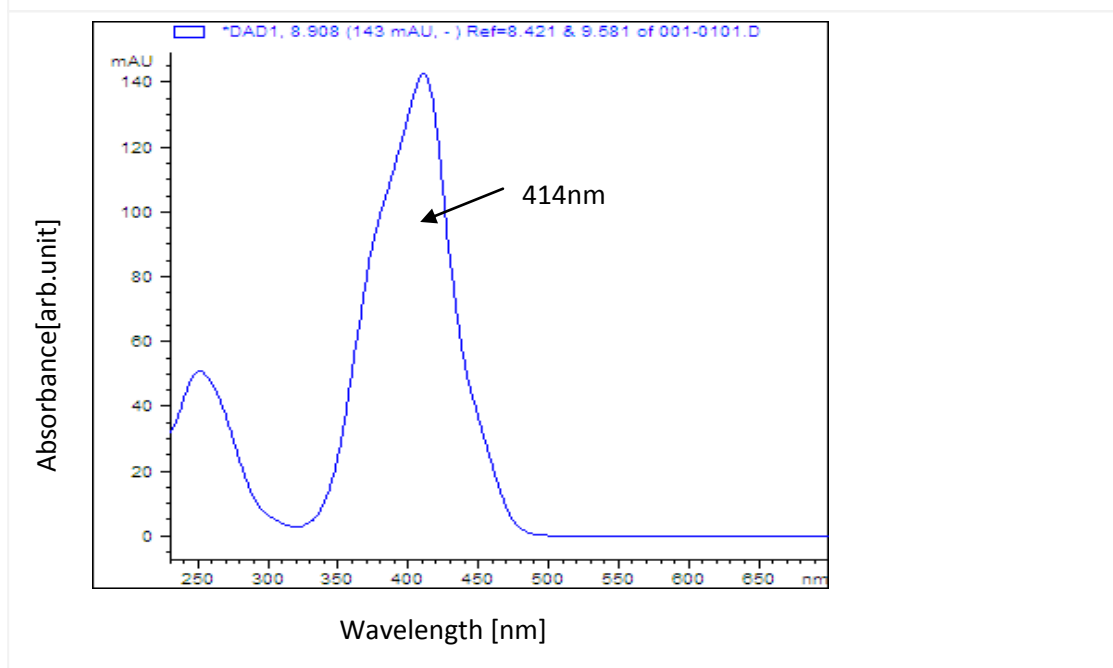
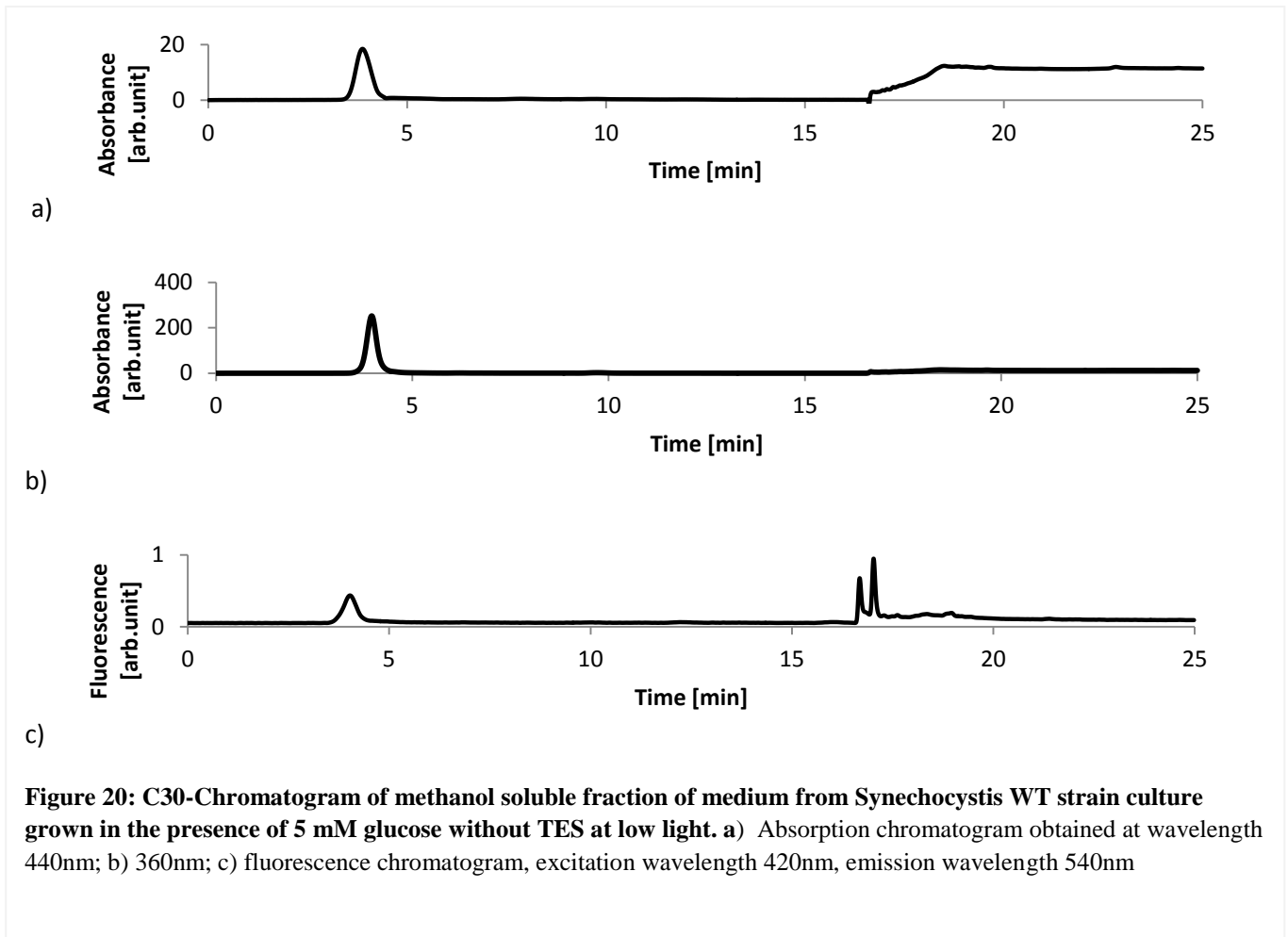
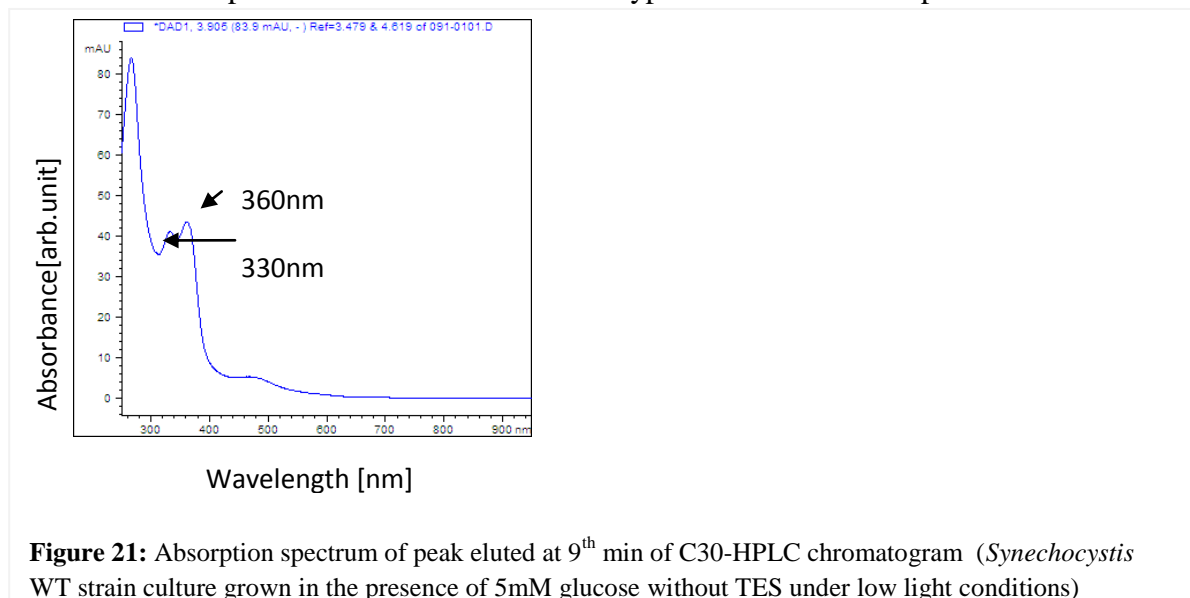


Figure 19: Absorption spectrum of peak at 9th min of C30-HPLC chromatogram
(*Synechocystis* WT strain culture grown in the presence of 5 mM glucose and 10 mM TES under low light conditions)

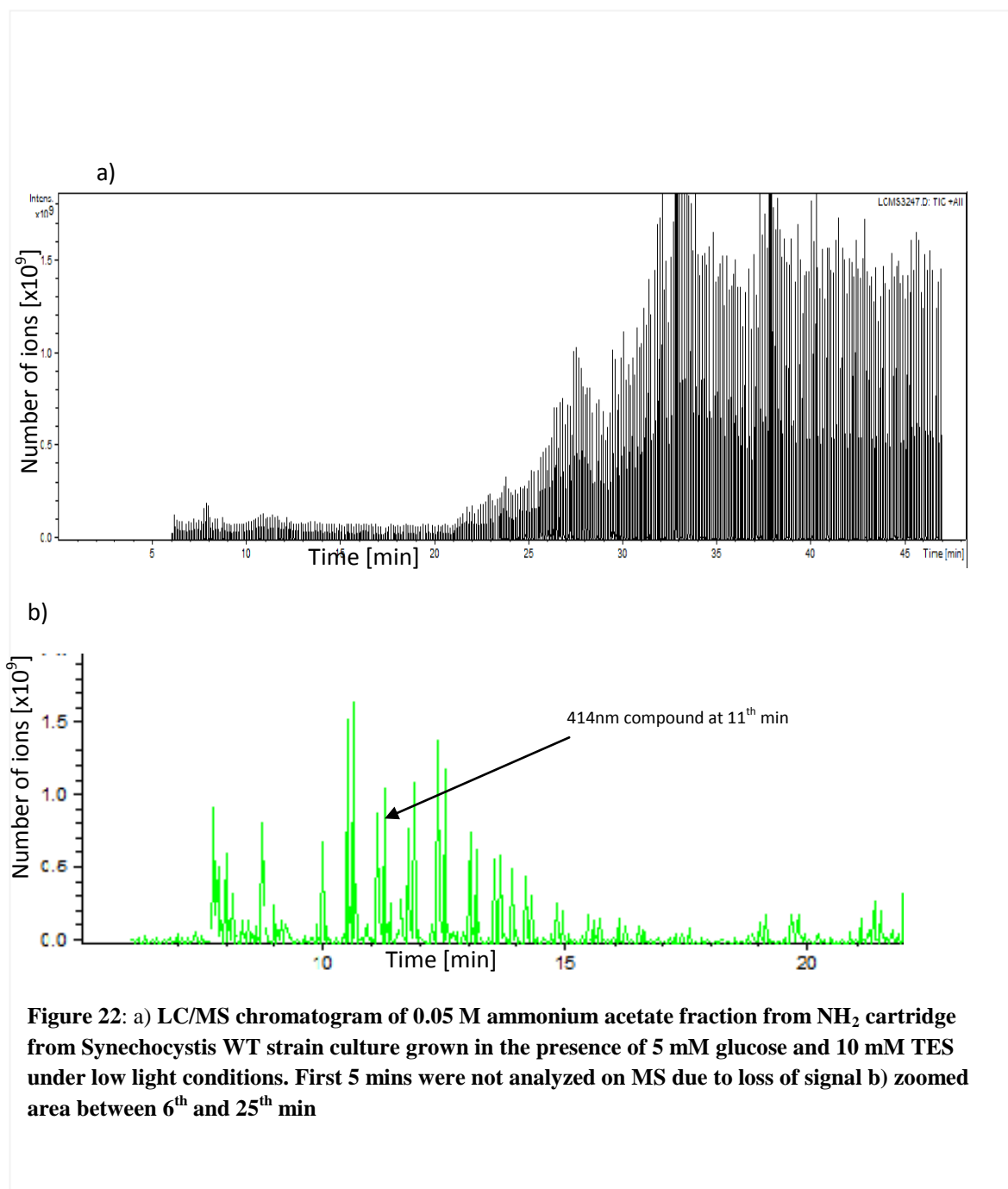
For comparison, the same experiment was repeated with sample from *Synechocystis* WT strain culture grown in presence of 5 mM glucose but without TES (Fig. 20).



The 360-330 nm compound eluted again at the very beginning of the elution at about 3rd min, but there was no peak between 9th and 15th min typical for 414 nm compound.

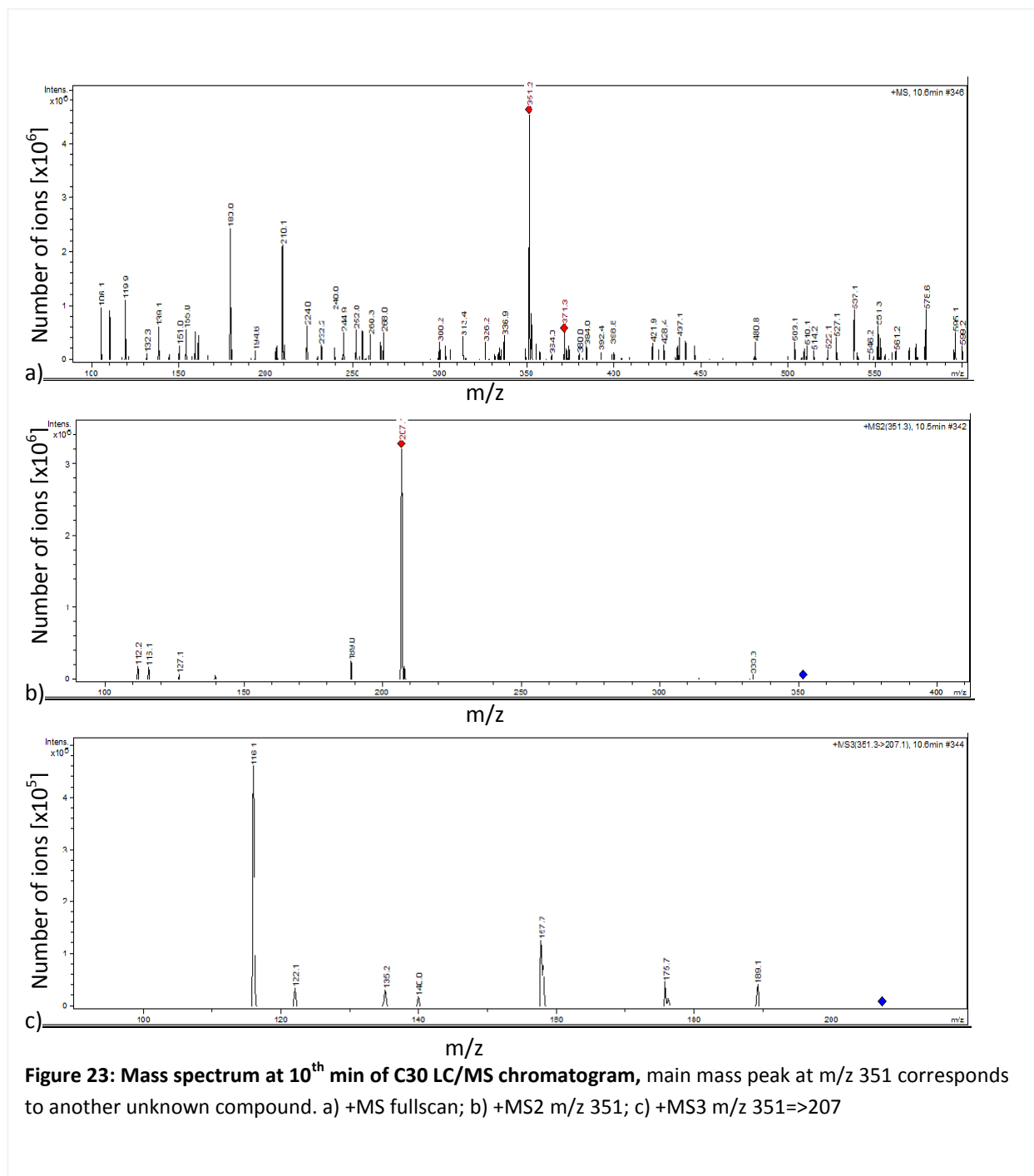


According to this result we concluded that the 414 nm compound could be separated from the 360-330 nm compound on C30 column. Nevertheless, it was necessary to check the purity of 8 min fraction also using MS detector. For this purpose we used the same column but we decreased the flow rate to 0.5 ml/min to increase the time for ionization. However, due to high concentration of unknown compound between 0-5 mins that caused loss of signal in MS instrument, only compounds after 6th min could be investigated (Fig. 22)



The 414 nm compound eluted at 11th min showed the m/z value 383 and gradually fragmented into m/z 355 and m/z 124 (Fig. 23), which corresponds to previously obtained highly resolved MS spectra (Komenda, unpublished, see Attachment 9.1).

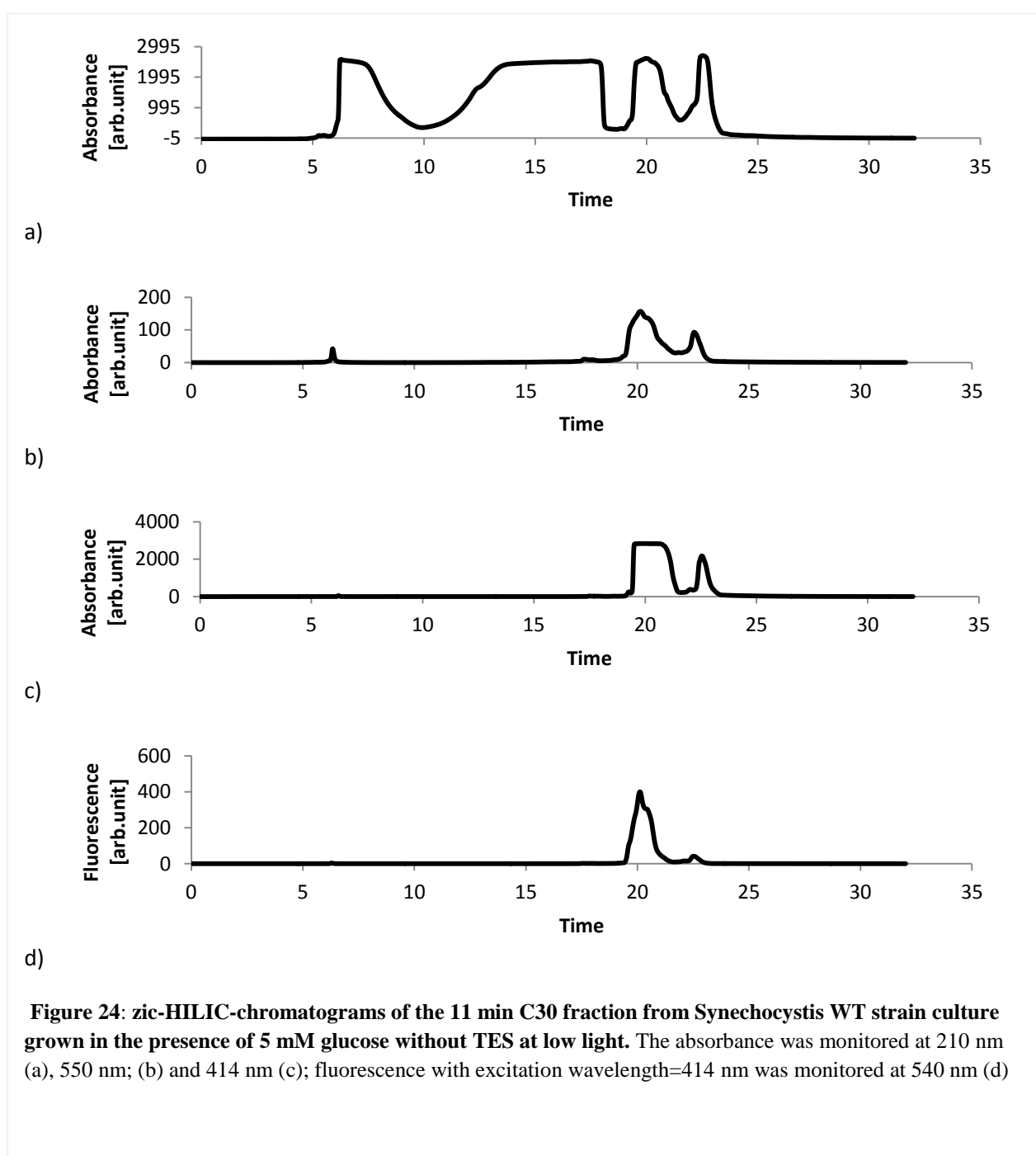
Besides the 414 nm compound there was another dominant compound continually eluted between 6th and 15th min with molecular ion at m/z 351 that fragmented into m/z 207.



So, the presence of this compound showed that separation by C30 column did not allow obtaining the 414 nm compound in the sufficient purity for NMR determination of its structure. From that reason we then tried to further purify the 414 nm compound-containing 11th min fraction by hydrophilic HPLC column.

3.4. Purification of the 414 nm compound by zic-HILIC HPLC column

In the final step, the 414 nm compound – containing 11th min fraction from the C30 column was further purified using zic-HILIC HPLC. The obtained chromatogram is shown in Fig. 24.



Thought previous purification on C30 column did not show a presence of large amount of the UV-absorbing substances in the 11th min fraction, its separation on HILIC column surprisingly resulted in two large UV-absorbing fractions eluted at around 8th and between 12th and 18th min (its spectrum see Fig. 25). These fractions did not absorb at 414 nm and therefore, we did not characterize them further. The 414 nm compound eluted at 20th min and was rather well separated from previous fractions (Fig. 24, its spectrum see Fig. 26). There was also yellow fraction eluted at 22.5th min with absorption spectrum having maxima at 430 nm and 270-290 nm. The 414 nm compound was collected, lyophilized and used for the NMR analysis.

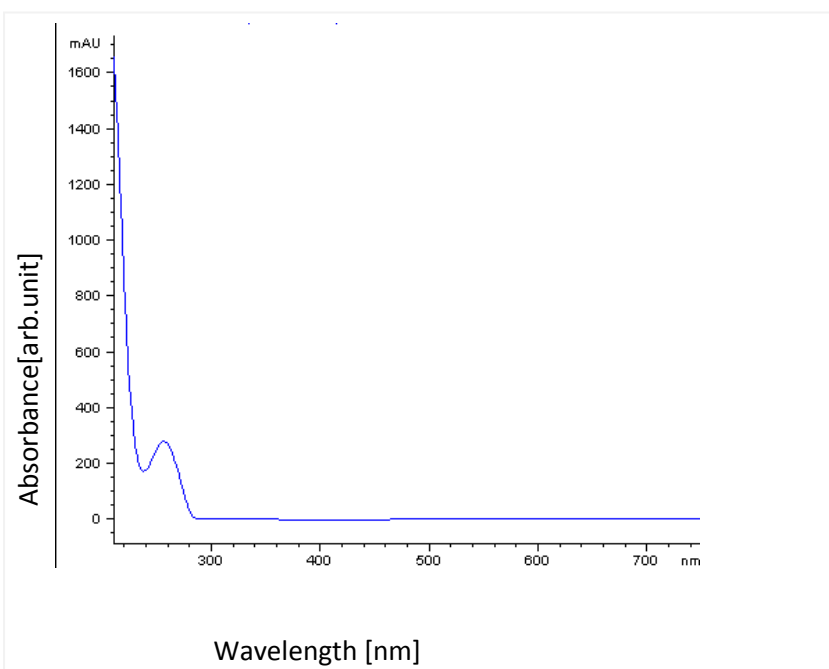


Figure 25: Absorption spectrum of fractions eluted from zic-HILIC column at 8th min.

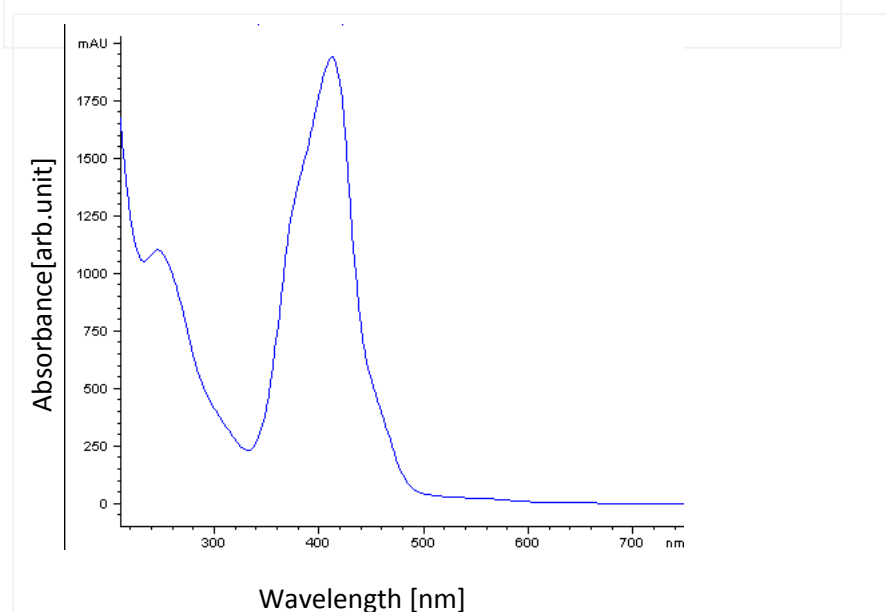
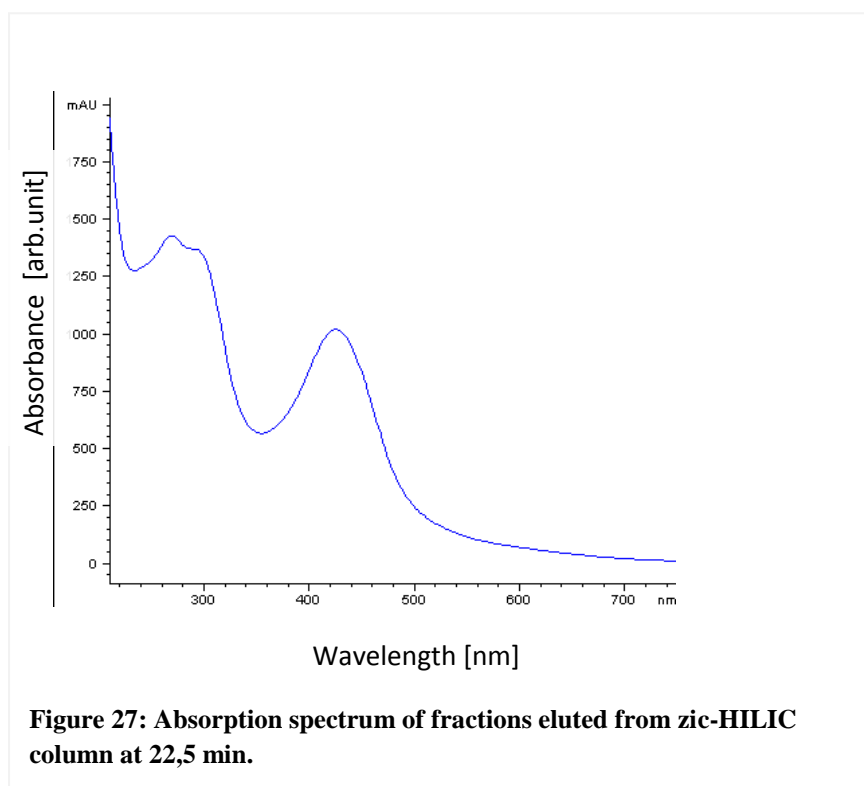


Figure 26: Absorption spectrum of fractions eluted from zic-HILIC column at 20th min corresponding to the 414 nm compound

Another compound elutes at 22.5th min with maximum absorbance at 450 nm (its spectrum on Fig. 27).

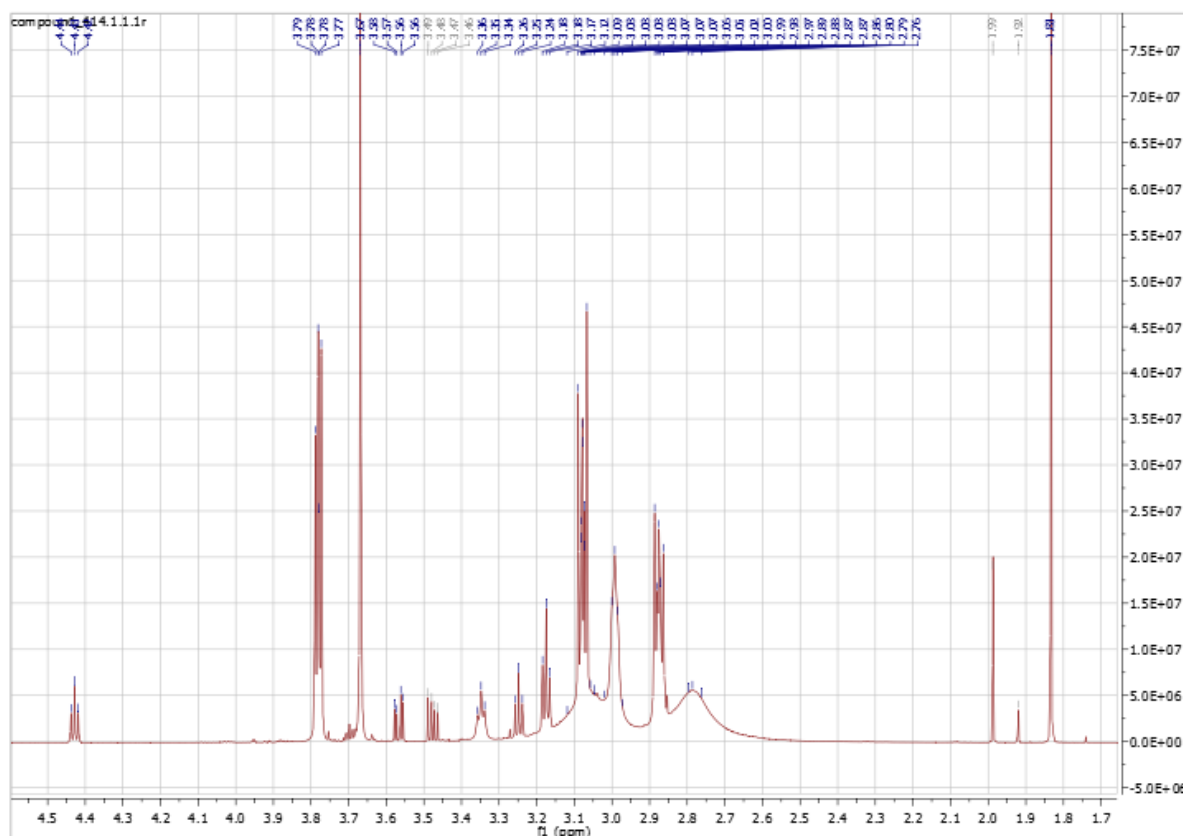


The main fraction at 20th min and minor fraction at 22.5th min were collected and lyophilized.

3.5. NMR Results

Fraction from zic HILIC column was used for measurement of the following NMR spectra: ^1H , ^{13}C , COSY, HSQC, HMBC (H-C) and HMBC (H-N). For all experiments D_2O was used as a solvent.

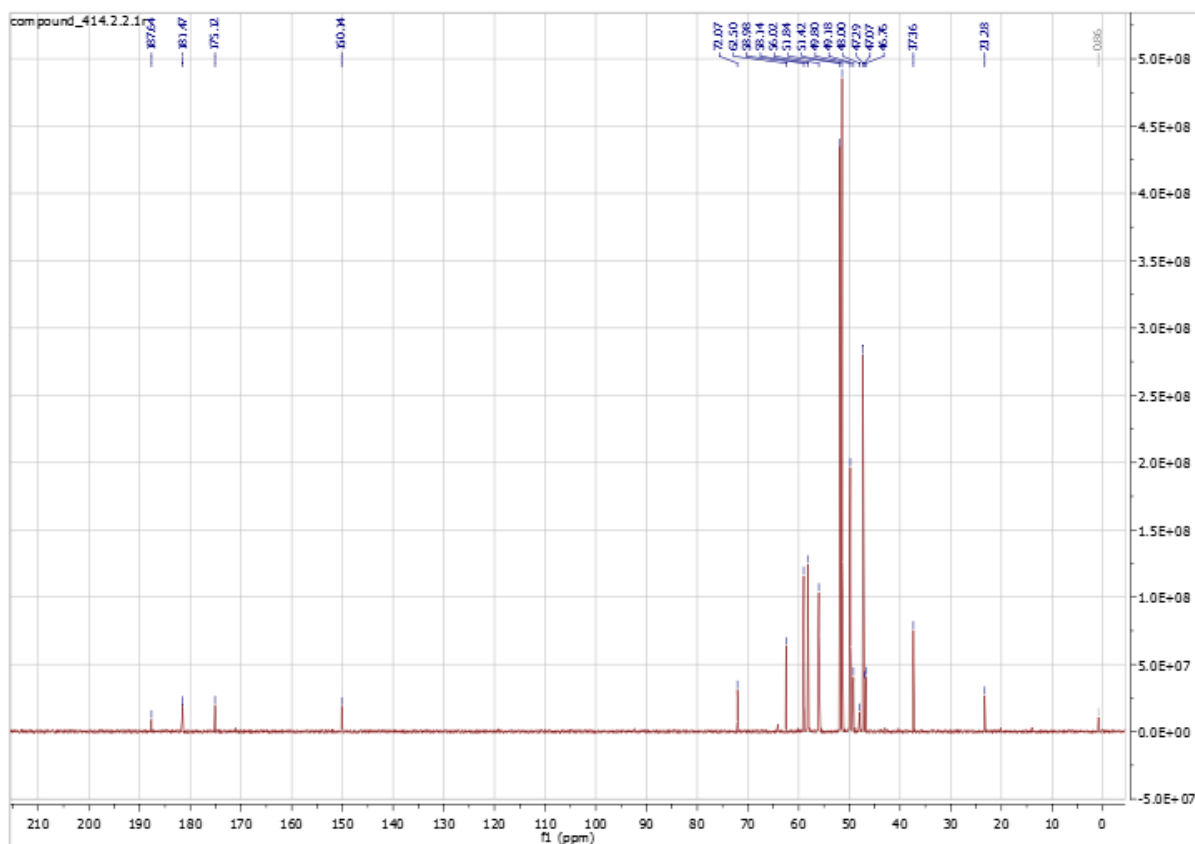
3.5.1. ^1H NMR Spectrum



	^1H -shift [ppm]	split	Integration	coupling constant [Hz]
1	2.87	multi	3,57	7
2	2.98	triplet	3,4	7
3	3.8	multi	4,26	7
4	3.18	triplet	1	7
5	3.25	triplet	0,5	7
6	3.35	triplet	0,6	7
7	3.47	quadruplet	0,18	7
8	3.57	quadruplet	0,18	7
9	3.67	singlet	2,14	7
10	3.78	triplet	3,4	7
11	4.43	triplet	0,24	7

Figure 28: ^1H NMR Spectrum of the 414 nm compound. Chemical shift are shown in the enclosed table

3.5.2. ¹³C NMR Spectrum



	¹³ C- shift		¹³ C- shift
1	37.24	10	56.00
2	46.74	11	58.12
3	47.03	12	58.93
4	47.25	13	62.53
5	48.00	14	72.08
6	49.16	15	150.09
7	49.83	16	175.09
8	51.38	17	181.48
9	51.81	18	187.65

Figure 29: ¹³C NMR Spectrum of the 414 nm compound. Chemical shift are shown in the enclosed table

3.5.3. COSY Spectrum

COSY interactions		
^1H [ppm]		^1H [ppm]
2.87	=>	3.8
2.98	=>	3.78
3.18	=>	3.35
3.25	=>	4.43
3.47	=>	3.57

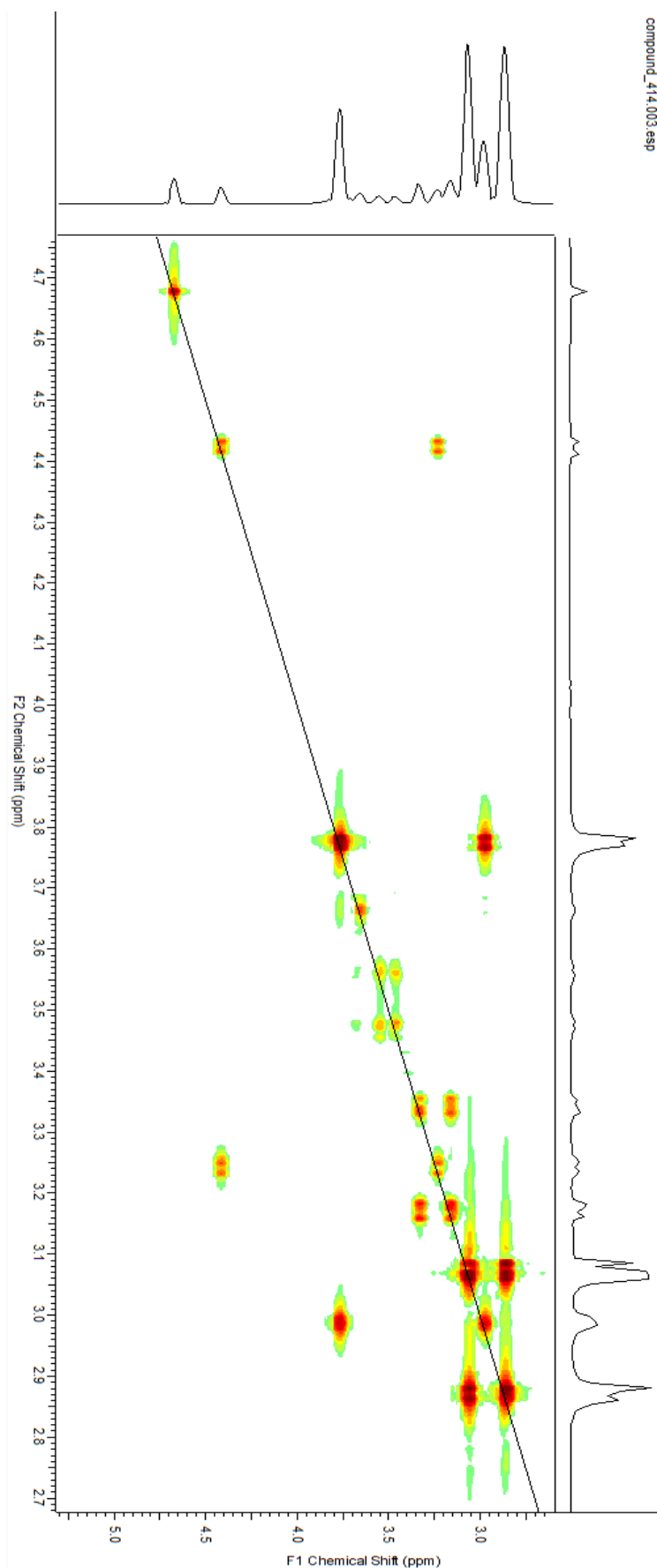


Figure 30: COSY NMR Spectrum of the 414 nm compound. Correlations are shown in the enclosed table

3.5.4. HSQC Spectrum

HSQC interaction		
^1H [ppm]		^{13}C [ppm]
2.87	=>	51.81
2.98	=>	58.12
3.8	=>	47.25
3.18	=>	48.00
3.25	=>	49.16
3.35	=>	37.24
3.67	=>	58.12
3.77	=>	49.74
3.78	=>	56.00
4.43	=>	47.03

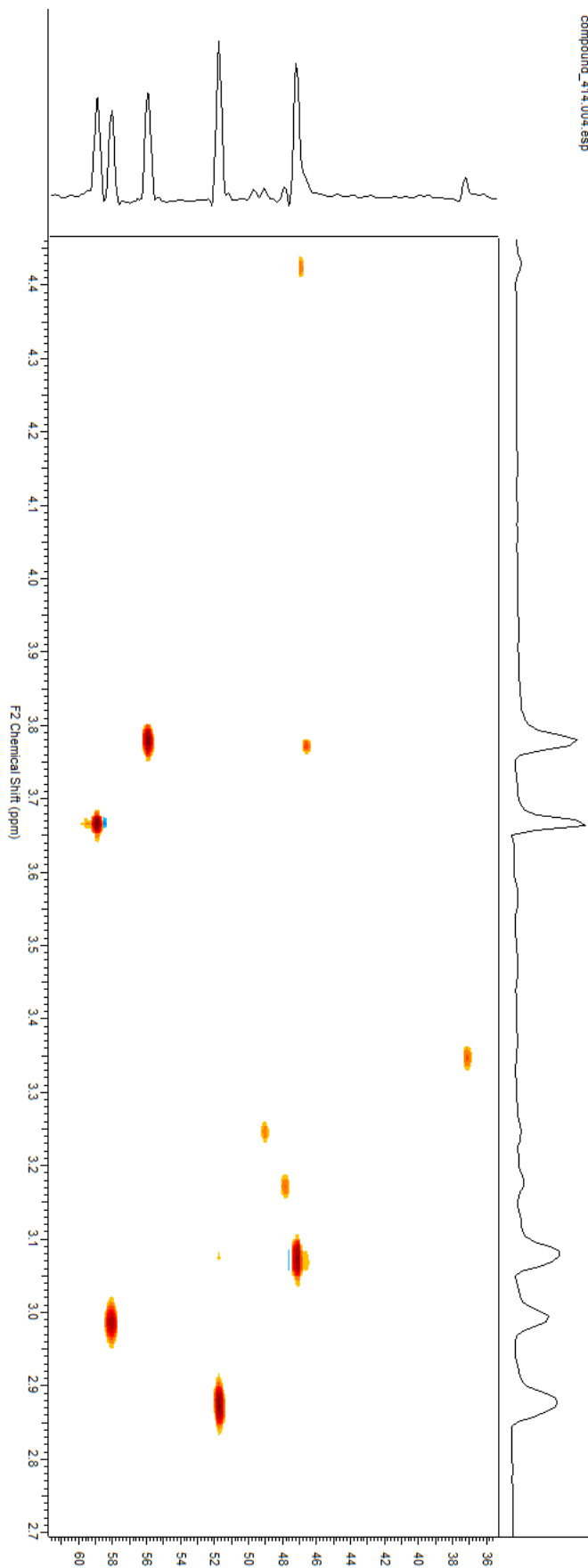


Figure 31: HSQC NMR Spectrum of the 414 nm compound. Correlation are shown in the enclosed table

3.5.5. HMBC (H-C) Spectrum

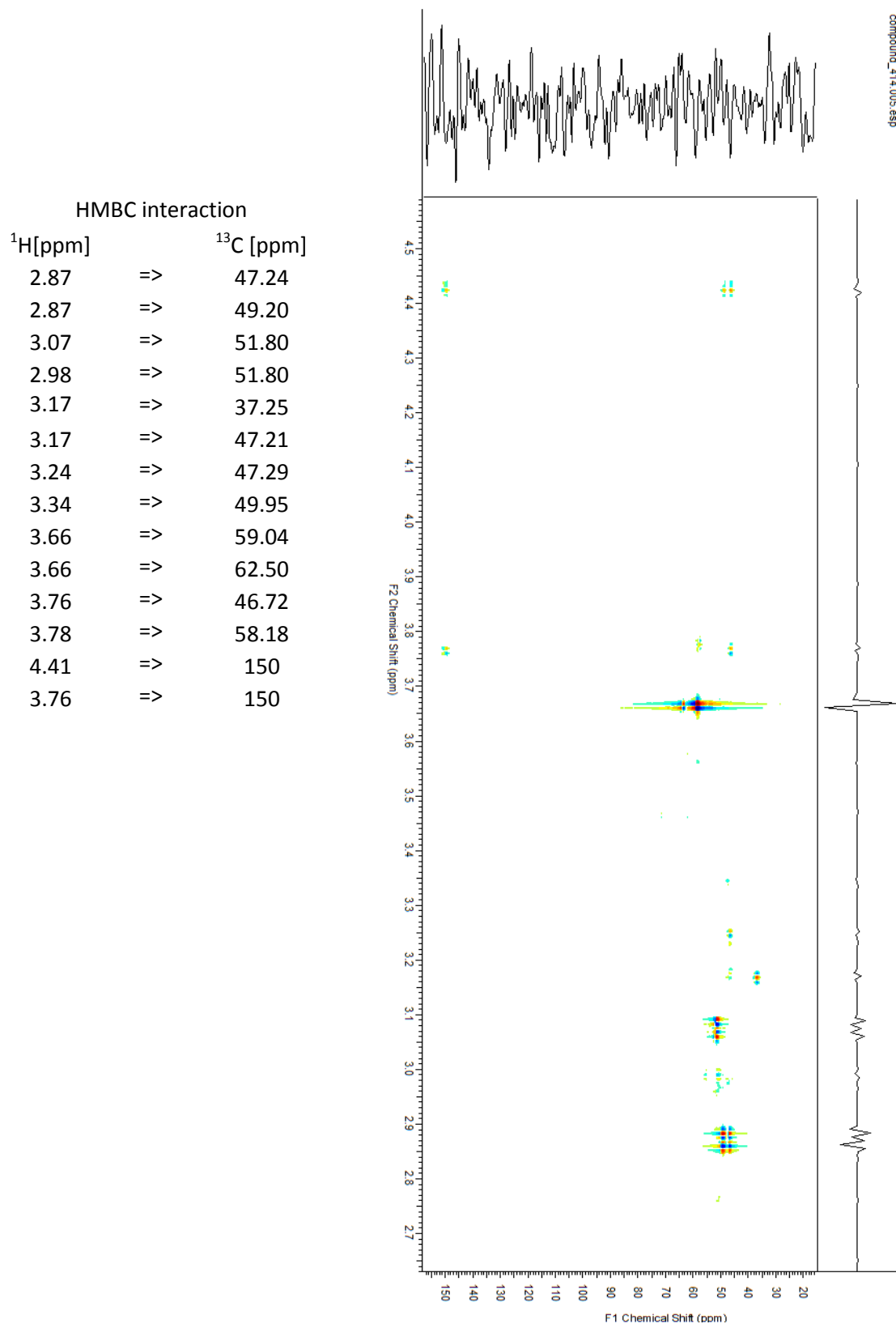


Figure 32: HMBC (¹H-¹³C) NMR Spectrum of the 414 nm compound. Correlation are shown in the enclosed table

3.5.6. HMBC (H-N) Spectrum

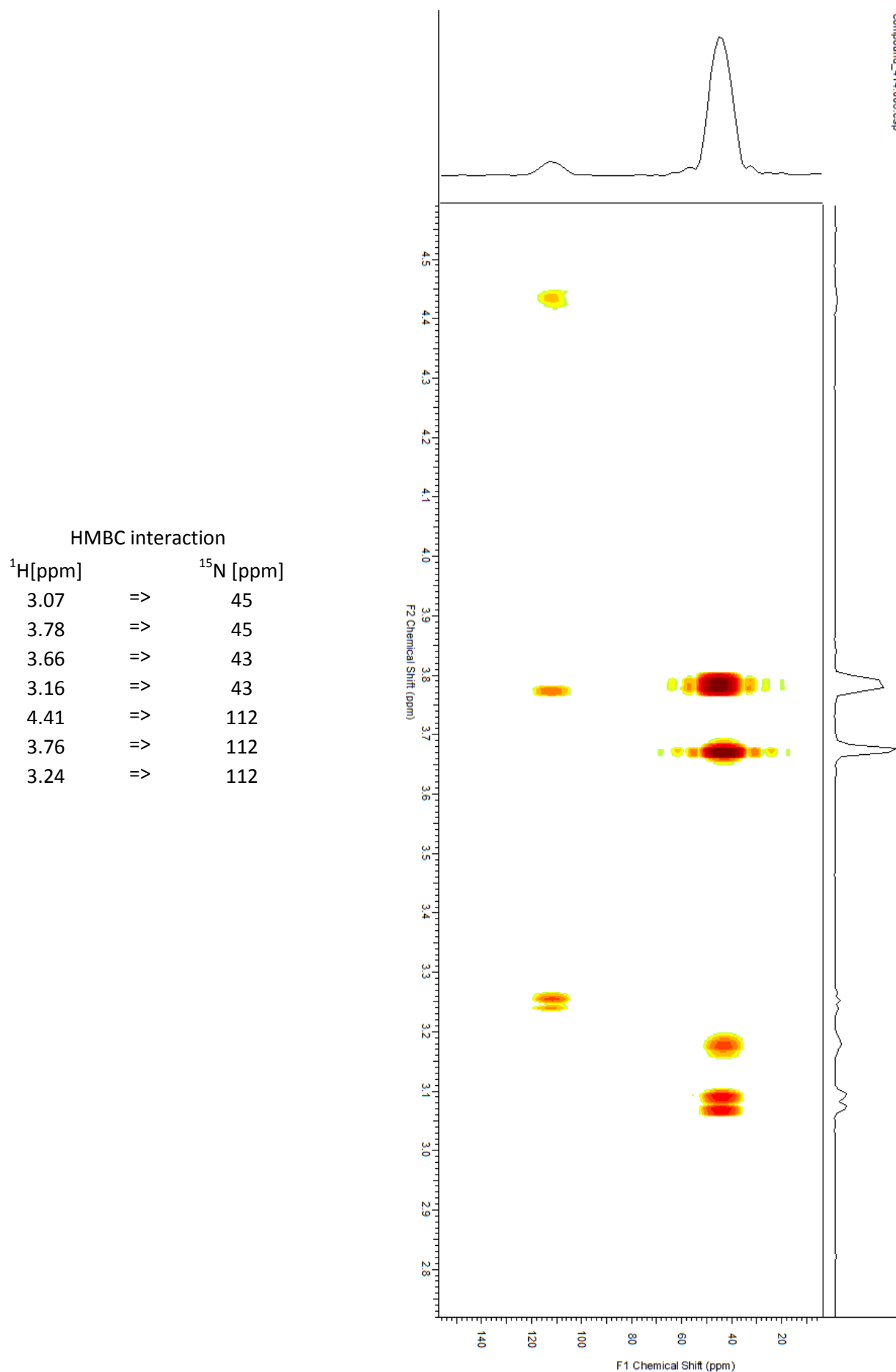


Figure 33: HMBC (¹H-¹⁵N) NMR Spectrum of the 414 nm compound. Correlation are shown in the enclosed table

3.6. Effect of TES buffer on the formation of the 414 nm in the cell-free medium

To judge whether the 414 nm compound can be formed in the cell-free medium obtained after cultivation of WT cells in the presence of glucose, we took the centrifuged medium, added 10 mM TES and incubated this cell-free mixture under low light conditions for 3 days. Then we compared the changes in the control TES-free medium and the TES-containing one by measurement of the absorption spectra (Fig. 34).

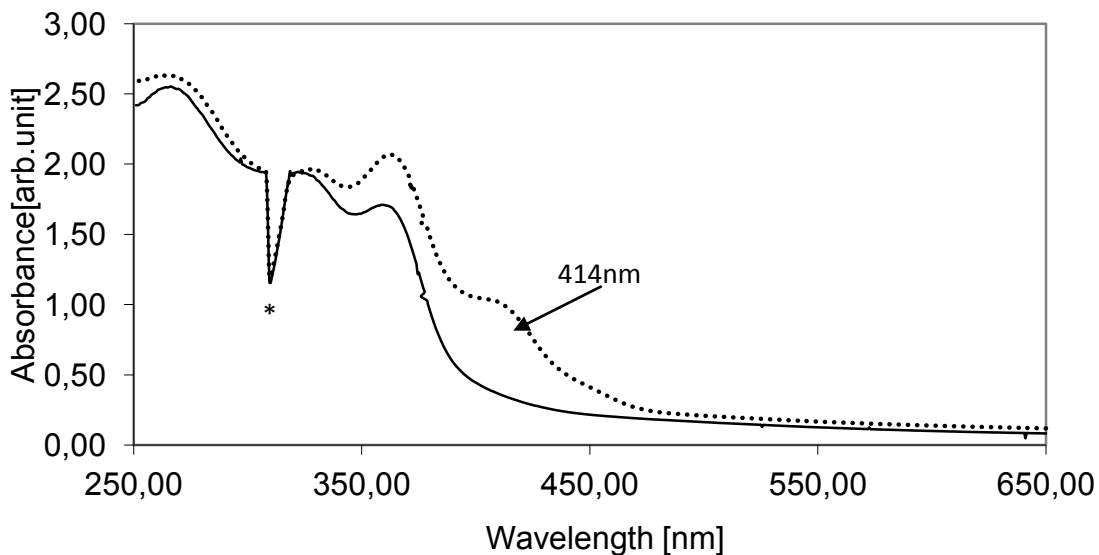


Figure 34: Comparison of absorption spectra of cultivation medium from the *Synechocystis* WT strain grown in the presence of 5 mM glucose subsequently incubated in the absence or the presence of TES.

Asterisk indicates the artefactual spike at 310nm caused by switch between the halogen and deuterium lamp. Continuous line: medium incubated without TES buffer for 3 days at low light; dashed line: the same medium after adding 10 mM TES buffer and incubation for 3 days at low light.

It became obvious that incubation of the medium with TES led to the formation of the 414 nm compound even in the absence of cells.

4. Discussion:

Structure of the 414 nm compound

The studied substances released from *Synechocystis* cells grown in the presence of glucose without TES were unstable in light and appeared in complex chromatographic fractions difficult to further purify. Therefore, we concentrated our effort on the purification and characterization of the compound generated in the medium in the presence of TES. Surprisingly, this so called 414 nm compound could be generated even without cells after addition of TES to the medium obtained after cultivation of cells in the presence of glucose under low light conditions. We speculate that this reaction was not spontaneous and was catalyzed by an unknown enzyme present in the medium. As seen in NMR spectra, the 414 nm compound purified by combination of SPE, hydrophobic and hydrophilic chromatography was almost pure, but the absence of aromatic carbons (= carbons with an NMR shift between 100 and 150 ppm) excluded its identity as a simple derivative of tetrapyrrole. This finding did not apparently confirm our initial working hypothesis based on similarity in absorption spectra between the excreted substances and plant chlorophyll degradation products.

The dependence of the compound formation on the presence of TES suggested that TES or its parts could be components of the compound. Indeed, some peaks in the NMR spectrum of the 414 nm compound corresponded well with the predicted NMR shifts of some TES atoms (Fig. 35). In the HMBC (^1H - ^{13}C) spectrum (Fig. 32), we distinguished 3 different nitrogen atoms with chemical shift 43 ppm, 45 ppm and 112 ppm. The nitrogen with a chemical shift 43 ppm correlated with hydrogens with chemical shift 3.66 ppm and 3.17 ppm, respectively. According to these values this nitrogen could be assigned to nitrogen originating from the TES molecule.

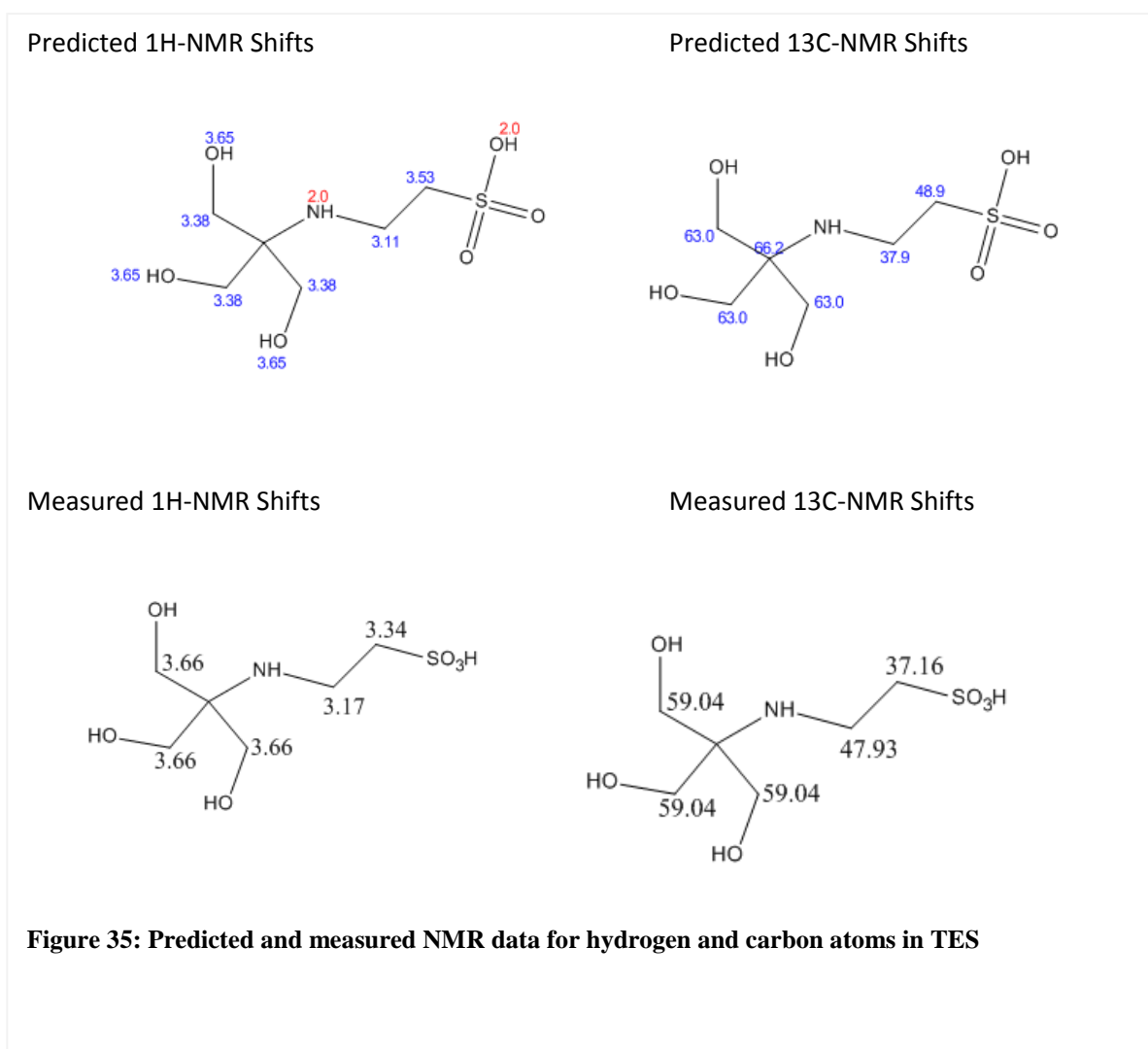


Figure 35: Predicted and measured NMR data for hydrogen and carbon atoms in TES

The second nitrogen with chemical shift 45 ppm showed strong correlation with hydrogen (shift 3.78 ppm) that is bound to carbon (shift 55.97 ppm) and hydrogen (shift 3.07 ppm) bound to another carbon with shift 47.33 ppm. Taking together with COSY data (Fig. 30), the second nitrogen appears to be bound within the fragment shown in Fig. 36.

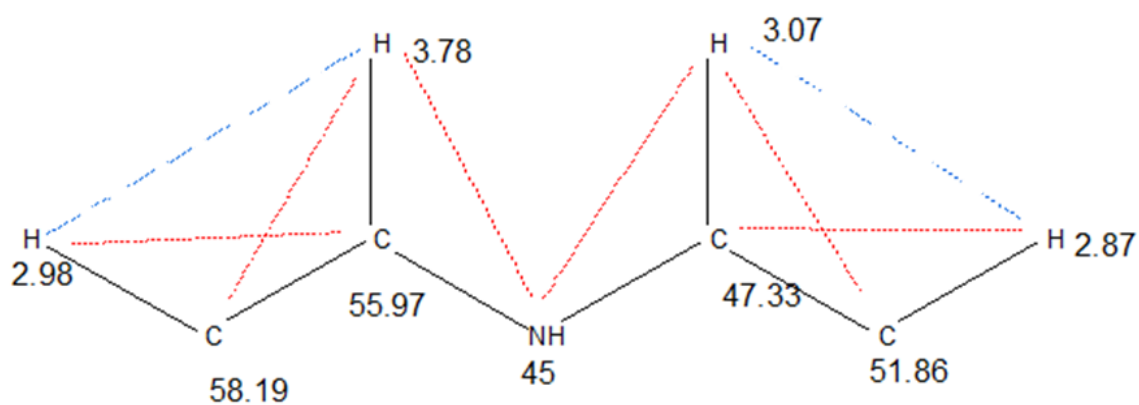


Figure 36: Fragment of the 414nm compound with appropriate NMR (dashed lines – COSY correlations, continuous lines – HMBC correlations)

The ^1H NMR further shows, that both hydrogens - 3.07 ppm and 2.87 ppm had a typical splitting for CH_2 groups as seen in Fig. 37.

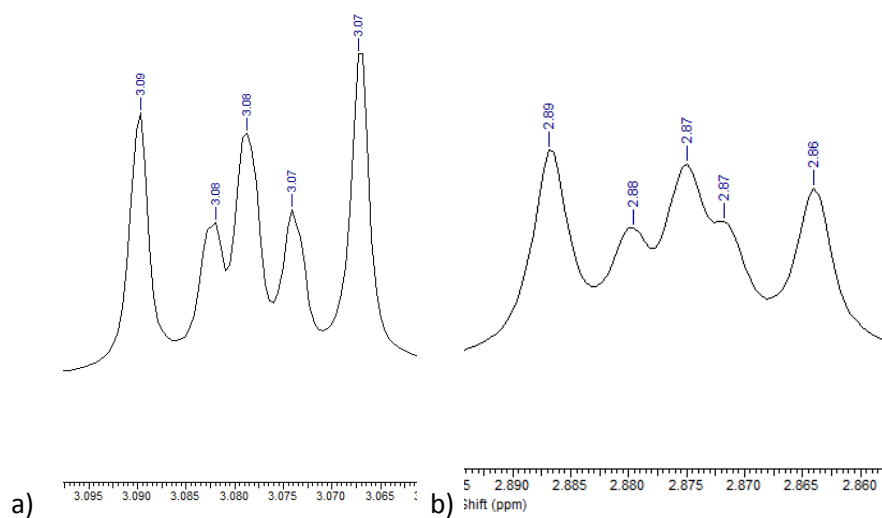


Figure 37: ^1H NMR Spectrum – splitting pattern of a) 3.08 ppm and b) 2.87 ppm peak

On this carbon chain there are no more correlations to other atoms.

The last nitrogen had chemical shift 112 ppm which is typical for primary amines and has correlation with hydrogen with chemical shift 2.98 ppm from previous fragment, 4.42 ppm and another one with chemical shift 3.76 ppm. As seen on Fig. 38, this hydrogen is not the same one as the hydrogen with chemical shift 3.78 ppm, although in $^1\text{H-NMR}$ spectrum there is almost no significance of this hydrogen. This hydrogen has relatively high correlation with carbon with chemical shift 150 ppm. According to these nitrogen and carbon

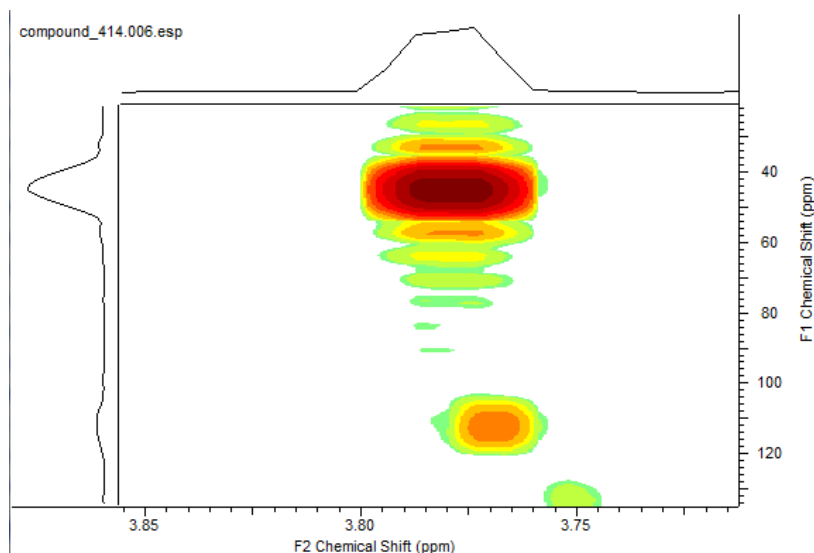


Figure 38: HMBC Spectrum, zoomed area of peaks 3.76 ppm and 3.78 ppm

correlation we can expand the fragment by four more carbon atoms as seen on Fig. 39.

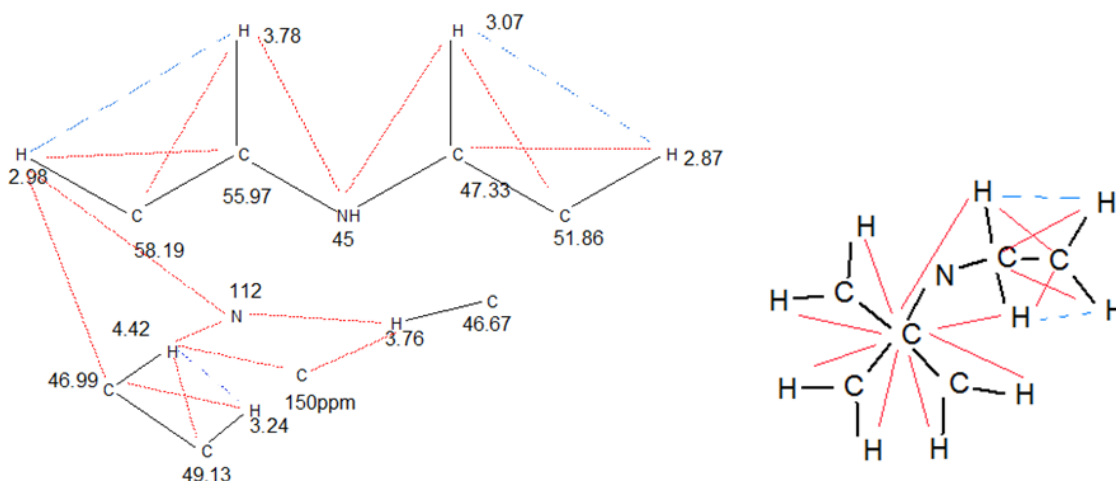


Figure 39: Fragment of 414 nm compound with appropriate NMR shifts (dashed lines – COSY correlations, continuous lines – HMBC correlations) and fragment of TES buffer

There are 3 more carbons with chemical shift 175, 181 and 188 ppm, but these carbons have no correlation in any spectra, so it is very hard to say, what type of carbon it is and where are these carbons connected.

However the compound is well soluble only in water therefore use of DMSO or similar solvents, which are more suitable for NMR, was not possible and we used D₂O as a solvent. Therefore, hydrogen bound in polar groups like OH or COOH were very fast exchanged with deuterium from the solvent and were no more visible in the magnetic field. Using DMSO or similar solvents that are more suitable for NMR characterization of carboxylic or alcohol hydrogens, led to lowering of all signals (the 414 nm compound from C30-HPLC diluted in DMSO is shown in Attachment 9.2).

The MS-Spectra of the 414 nm compound shows the molecular ion with m/z 383 Da and 3 aldehyde groups (loss 29 Da). These aldehydes could be on three carbons with the highest chemical shift. According to M+H mass, the composition of 414 nm compound should be C₁₁H₁₄N₂S₂O₉, but on ¹³C NMR there are 18 different carbons and 3 nitrogens. Either the sample was still not pure, or there was some fragmentation in MS-Source, and the molecular ion with m/z 383 is only a fragment of a bigger compound, but we were not able to prove this theory. However concerning the known fragment we are still not able to explain, why the 414 nm compound is yellow and why it has such a high fluorescence. Similar fluorescence has for example some fulgides or proteins³¹.

Concerning the compound with maximum absorbance at 360 nm and 330 nm we did not investigate its structure, but according to absorption we can speculate that this compound could be excreted during the growth as UVA - protecting agent similarly as carotenoids.

Role of TES-buffer

Our results clearly proved that the presence of TES is essential for the formation of the 414 nm compound. It means that TES reacts, most probably under the assistance of unknown enzyme(s), with a metabolic product of *Synechocystis* - this is rather surprising since TES belongs to so called Good's buffers that are supposed to be biologically inert and should not be easily metabolized. Addition of TES buffer to centrifuged medium and incubation of this sample on LL leads to a formation of the same compound as growth of

Synechocystis cells with TES. The 414nm compound could be therefore some simple partial chemical modification of original 360-330 compound, but we could not prove it due to our inability to sufficiently purify this compound and due to its light sensitivity. During our experiments we also had to cope with some variability in the rate of formation of both the 360-330 nm as well as the 414 compounds by cyanobacterial cells. Under certain circumstances (for instance when the cultivation room was changed or new cultivation medium was made) the formation of the compounds became occasionally very limited but we were not able to determine the real reason for it. A possible explanation would be a use of chemicals with undefined impurities that was important for or inhibited the formation of the compounds, or a change in the cultivation conditions due to the ongoing reconstruction of the Department of phototrophic microorganisms (differences in temperature or its stability, CO₂ content etc).

5. Conclusions

We confirmed that cultivation of the cyanobacterium *Synechocystis* sp. PCC 6803 under low light conditions in presence of TES buffer and glucose leads to production of yellow compound with the main absorption maximum at 414 nm. We showed that its formation requires the presence of TES and we successfully purified the compound using SPE, C30 and HILIC HPLC. Although we were able to measure both MS and NMR spectra, we were not able to determine the final structure. This was partly caused by apparently complicated nature of the compound and partly by its very polar character which caused its low solubility in other solvents than water. This precluded obtaining essential information on the location of alcohol and other polar groups within the structure.

6. Abbreviation

CAPS	N-cyclohexyl-3-aminopropanesulfonic acid
COSY	Correlation spectroscopy
ESI	Electrospray Ionization
HMBC	Heteronuclear Multiple Bond Correlation spectroscopy
HPLC	high performance liquid chromatography
HSQC	Heteronuclear single quantum coherence spectroscopy
LL	low light (5 $\mu\text{mol photons m}^{-1} \text{s}^{-1}$)
MALDI	Matrix-assisted laser desorption/ionization
MES	2-(N-morpholino)ethanesulfonic acid
MS	Mass spectroscopy
NCCs	non-fluorescent chlorophyll catabolites
NDH	NAD(P)H dehydrogenase
NL	normal light (40 $\mu\text{mol photons m}^{-1} \text{s}^{-1}$)
PC	plastocyanin
pFCC	primary fluorescent chlorophyll catabolite
PQ	plastoquinone
PS I	Photosystem I
PS II	Photosystem II
RCC	red chlorophyll catabolite
SDH	succinate dehydrogenase
TES	(2-[[1,3-dihydroxy-2-(hydroxymethyl)propan-2-yl]amino]ethanesulfonic acid.)
WT	Wild type strain

7. Acknowledgment

The presented Master Thesis was performed at the Department of phototrophic microorganisms of the Institute of Microbiology, ASCR

The NMR spectra were recorded at the Laboratory of Molecular Structure Characterization of Institute of Microbiology, ASCR.

The NMR spectra were recorded at the NMR center of the Universities of Linz and South Bohemia with support from the European Union through the EFRE INTERREG IV ETC-AT-CZ programme (project M00146 “RERI-uasb”).

The MALDI-TOF MS spectra were recorded at the Laboratory of Molecular Structure Characterization of Institute of Microbiology, ASCR.

8. Literature

- 1) SCHOPF, J. William; KUDRYAVTSEV Anatoliy B.; AGRESTI, David G.; WDOWIAK, Thomas J. and CZAJA, Andrew D. Laser-Raman imagery of Earth's earliest fossils. *Nature*. 2002, 416, 6876, p. 73-76. ISSN 0028-0836. DOI: 10.1038/416073a. Available online: <http://www.nature.com/doi/10.1038/416073a>
- 2) STANIER, R. Y., et al. Purification and properties of unicellular blue-green algae (order Chroococcales). *Bacteriological Reviews*, 1971, 35, 2, p. 171-205. ISSN 0005-3678
- 3) KEGG GENOME: Synechocystis sp. PCC 6803. KANEHISA LABORATORIES [online]. [cit. 2013-02-17]. Available online: http://www.genome.jp/kegg-bin/show_organism?org=syn
- 4) KHATTAR, J.; SINGH, D. and KAUR, Gurpreet. *Algal biology and biotechnology*. New Delhi: I.K. International Pub. House, c2009, p. 3-5. ISBN 978-938-0026-190.
- 5) HOICZYK, E. and HANSEL, A. Cyanobacterial Cell Walls: News from an Unusual Prokaryotic Envelope. *Journal of Bacteriology*. 2000, 182, 5, p. 1191-1199. ISSN 0021-9193. DOI: 10.1128/JB.182.5.1191-1199.2000. Available online: <http://jb.asm.org/cgi/doi/10.1128/JB.182.5.1191-1199.2000>
- 6) GLAUNER, B.; HÖLTJE, J. V. and SCHWARZ, Uli. The composition of the murein of *Escherichia coli*. *Journal of Biological Chemistry*, 1988, 263, 21, p. 10088-10095. ISSN 0021-9258
- 7) JÜRGENS, U. J.; DREWS, G. and WECKESSER, J. Primary structure of the peptidoglycan from the unicellular cyanobacterium *Synechocystis* sp. strain PCC 6714. *Journal of bacteriology*, 1983, 154, 1, p. 471-478. ISSN 0021-9193.
- 8) SAFI, Carl; CHARTON, Michael; PIGNOLET, Olivier; SILVESTRE, Françoise; VACA-GARCIA, Carlos and PONTALIER, Pierre-Yves. Influence of microalgae cell wall characteristics on protein extractability and determination of nitrogen-to-protein conversion factors: News from an Unusual Prokaryotic Envelope. *Journal of Applied Phycology*. 2013, 25, 2, p. 523-529. ISSN 0921-8971. DOI: 10.1007/s10811-012-9886-1. Available online: <http://link.springer.com/10.1007/s10811-012-9886-1>
- 9) Cyanobacteria: TutorVista.com. TUTORVISTA.COM [online]. [cit. 2013-02-17]. Available online: <http://www.tutorvista.com/content/biology/biology-iii/kingdoms-living-world/cyanobacteria.php>

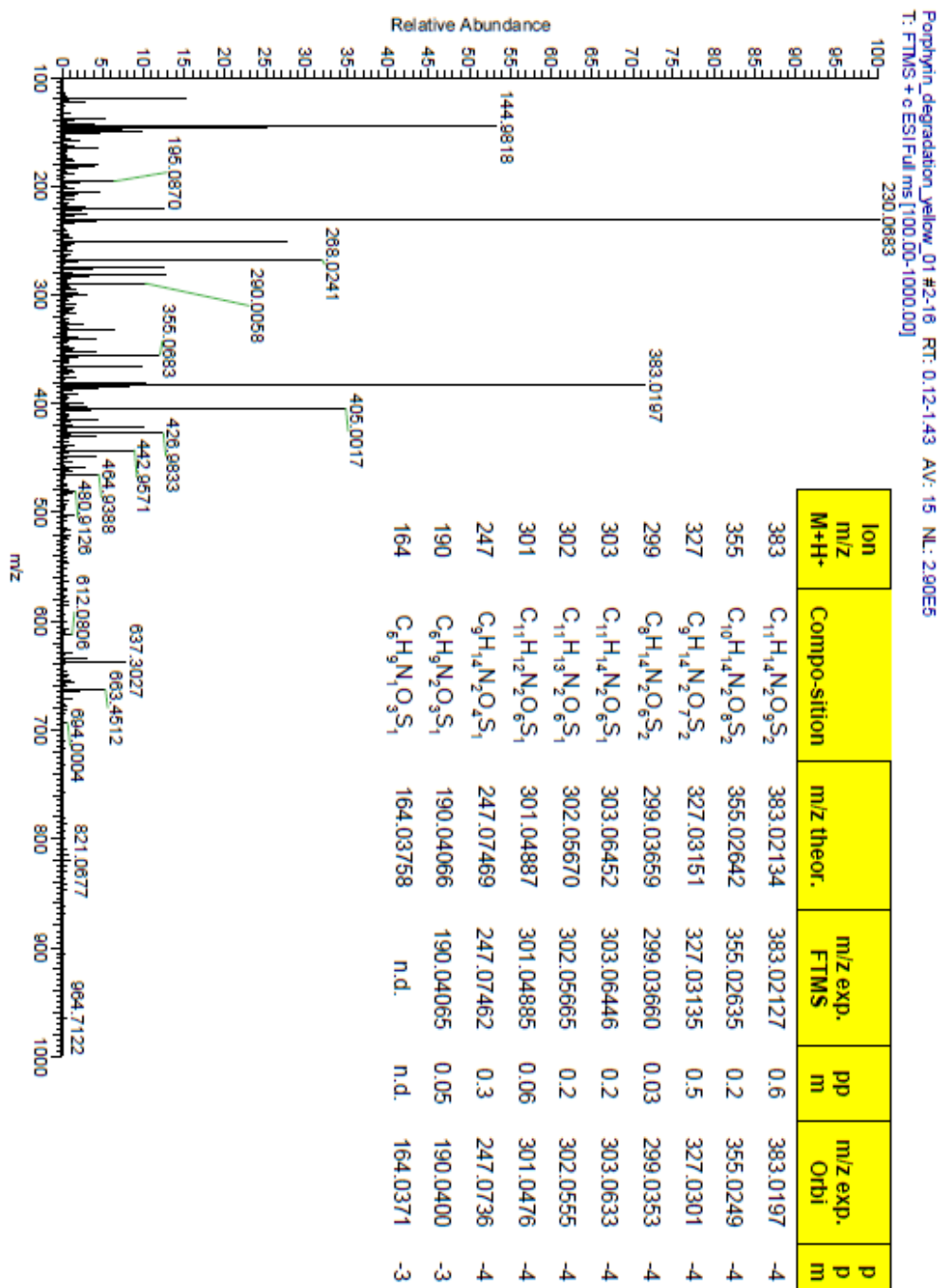
- 10) PESCHEK, Günter A. *Photosynthesis and Respiration of Cyanobacteria*. The Phototrophic Prokaryotes. Boston, MA: Springer US, 1999, 201 p. DOI: 10.1007/978-1-4615-4827-0_24. Available online: http://www.springerlink.com/index/10.1007/978-1-4615-4827-0_24
- 11) MICROBIOLOGY AND MOLECULAR BIOLOGY REVIEWS. Chlorophyll Fluorescence Analysis of Cyanobacterial Photosynthesis and Acclimation: Cyanobacterial thylakoid electron transport [online]. [cit. 2013-02-17]. Available online: <http://mmbr.asm.org/content/62/3/667/F1.large.jpg>
- 12) EMBL-EBI. Phycobilisome, alpha/beta subunit (IPR012128) [online]. [cit. 2013-02-17]. Available online: <http://www.ebi.ac.uk/interpro/IEntry?ac=IPR012128>
- 13) VINYARD, David J.; ANANYEV, Gennady M. and DISMUKES, G. Charles. Photosystem II: The Reaction Center of Oxygenic Photosynthesis. *Annual Review of Biochemistry*. 2013, 82, 1. ISSN 0066-4154. DOI: 10.1146/annurev-biochem-070511-100425. Available online: <http://www.annualreviews.org/doi/abs/10.1146/annurev-biochem-070511-100425>
- 14) UMENA, Yasufumi, et al. Crystal structure of oxygen-evolving photosystem II at a resolution of 1.9 Å. *Nature*, 2011, 473, 7345, p. 55-60. ISSN 0028-0836
- 15) VERMAAS, Wim F. J.; ANANYEV, Gennady M. and DISMUKES, G. Charles. Photosynthesis and Respiration in Cyanobacteria: The Reaction Center of Oxygenic Photosynthesis. *Annual Review of Biochemistry*. 2013, 82, 1. ISSN 0066-4154. DOI: 10.1038/npg.els.0001670. Available online: <http://doi.wiley.com/10.1038/npg.els.0001670>
- 16) CARR, N. and WHITTON, Brian A. *The Biology of cyanobacteria*. Berkeley: University of California Press, 1982, p. 195-205. ISBN 0520047176.
- 17) SCHERER, Siegfried; ALMON, Helmar and BÖGER, Helmar. Interaction of photosynthesis, respiration and nitrogen fixation in cyanobacteria. *Photosynthesis Research*. 1988, 15, 2, p. 95-114. ISSN 0166-8595. DOI: 10.1007/BF00035255. Available online: <http://link.springer.com/10.1007/BF00035255>
- 18) OOLEY, J. W.; VERMAAS, W. F. J. and BÖGER, Peter. Succinate Dehydrogenase and Other Respiratory Pathways in Thylakoid Membranes of *Synechocystis* sp. Strain PCC 6803: Capacity Comparisons and Physiological Function. *Journal of Bacteriology*. 2001, 183, 14, p. 4251-4258. ISSN 0021-9193. DOI: 10.1128/JB.183.14.4251-4258.2001. Available online: <http://jb.asm.org/cgi/doi/10.1128/JB.183.14.4251-4258.2001>

- 19) CLEA-SMITH, D. J.; ROSS, N.; ZORI, M.; BENDALL, D. S.; DENNIS, J. S.; SCOTT, S. A.; SMITH A. G. and HOWE, C. J. Thylakoid terminal oxidases are essential for the cyanobacterium *Synechocystis* sp. PCC 6803 to survive rapidly changing light intensities: Capacity Comparisons and Physiological Function. *Plant Physiology*. 2013, 183, 14. 34 p. ISSN 0032-0889. DOI: 10.1104/pp.112.210260. Available online: <http://www.plantphysiol.org/cgi/doi/10.1104/pp.112.210260>
- 20) Light Switchable Promoter. TU MUNICH [online]. [cit. 2013-02-17]. Available online: http://2012.igem.org/Team:TU_Munich/Project/Light_Switchable_Promoter
- 21) Structure of Phycocyanobilin. WIKIPEDIA COMMONS [online]. [cit. 2013-02-17]. Available online: <https://commons.wikimedia.org/wiki/File:Phycocyanobilin2.svg>
- 22) BUSCH, Andrea W.U.; REIJERSE, Edward J.; LUBITZ, Wolfgang; FRANKENBERG-DINKEL, Nicole and HOFMANN, Eckhard. Structural and mechanistic insight into the ferredoxin-mediated two-electron reduction of bilins. *Biochemical Journal*. 2011, Vol. 439, n. 2, p. 257-264. ISSN 0264-6021. DOI: 10.1042/BJ20110814. Available online: <http://www.biochemj.org/bj/439/bj4390257.htm>
- 23) KÜPPER, Hendrik; ANDRESEN, Elisa; WIEGERT, Susanna; ŠIMEK, Miloslav; LEITENMAIER, Barbara and ŠETLIK, Ivan. Reversible coupling of individual phycobiliprotein isoforms during state transitions in the cyanobacterium *Trichodesmium* analysed by single-cell fluorescence kinetic measurements. *Biochimica et Biophysica Acta (BBA) - Bioenergetics*. 2009, Vol. 1787, 3, p. 155-167. ISSN 00052728. DOI: 10.1016/j.bbabi.2009.01.001. Available online: <http://linkinghub.elsevier.com/retrieve/pii/S0005272809000085>
- 24) Structure and Reactions of Chlorophyll. JAMES STEER [online]. [cit. 2013-04-17]. Available online: <http://www.ch.ic.ac.uk/local/projects/steer/cloroads.gif>
- 25) Herbicide Mode of Action: Pigment Biosynthesis Inhibitors. BOB HARTZLER [online]. [cit. 2013-02-17]. Available online: http://www.agron.iastate.edu/courses/Agron317/Pigment_Inhibitors.htm
- 26) HÖRTENSTEINER, S. Chlorophyll breakdown in higher plants and algae. *Cellular and Molecular Life Sciences (CMLS)*. 1999, Vol. 56, 3-4, p. 330-347. ISSN 1420-682x. DOI: 10.1007/s000180050434. Available online: <http://link.springer.com/10.1007/s000180050434>
- 27) RÜCKMANN, I; ZEUG, A.; VON FEILITZSCH, T. and RÖDER, B. Orientational relaxation of pheophorbide-a molecules in the ground and in the first excited state

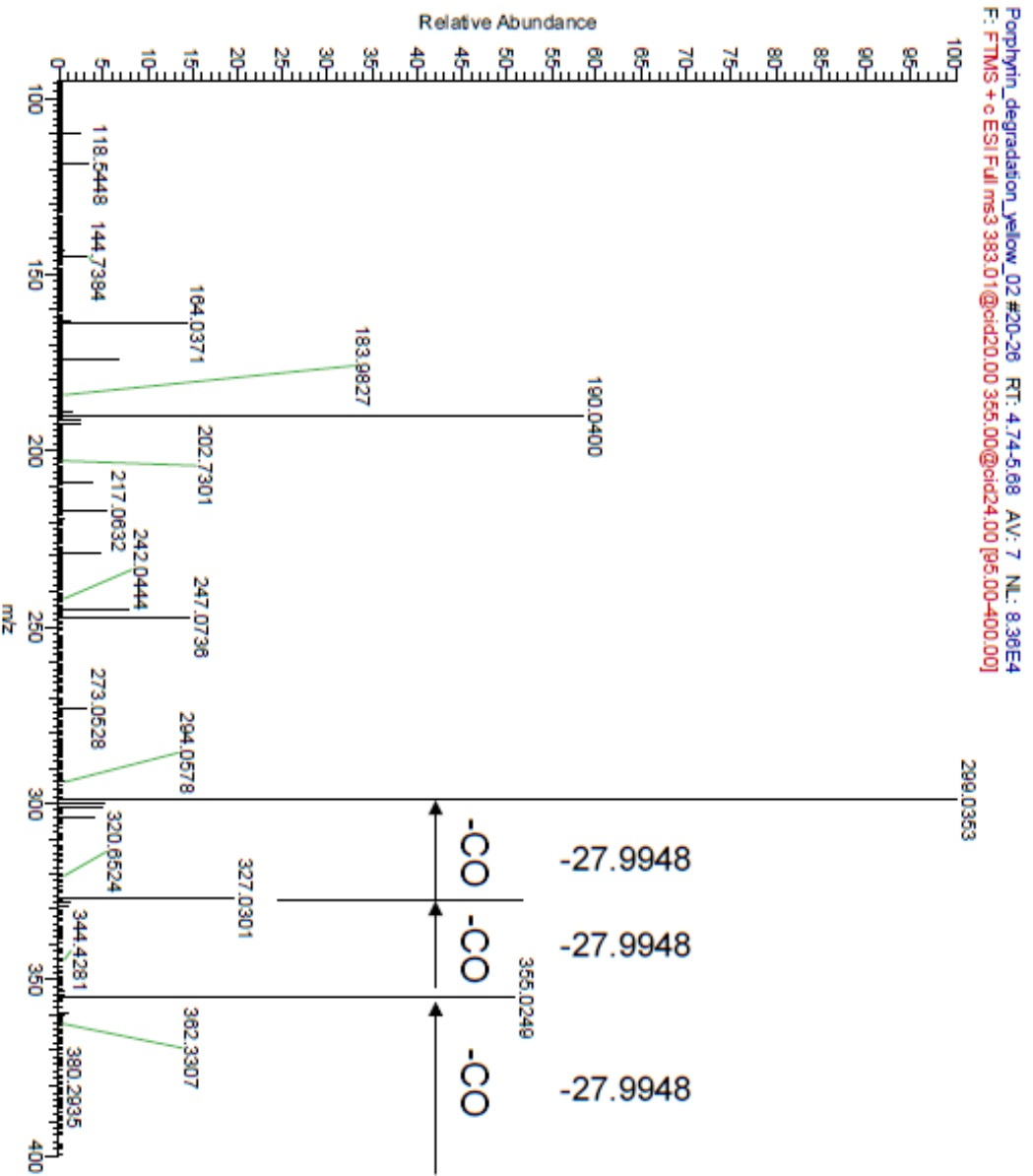
- measured by transient dichroism spectroscopy. *Optics Communications*. 1999, Vol. 170, 4-6, p. 361-372. ISSN 00304018. DOI: 10.1016/S0030-4018(99)00488-5.
Available online: <http://linkinghub.elsevier.com/retrieve/pii/S0030401899004885>
- 28) Pentose Phosphate Pathway. RICHARD A. PASELK [online]. [cit. 2013-04-17].
Available online:
<http://users.humboldt.edu/rpasek/C431.F07/C431Notes/C431nLec34.htm>
- 29) KOMENDA, Josef and SOBOTKA, Roman. Unpublished results
- 30) HERDMAN, Michael, et al. Deoxyribonucleic acid base composition of cyanobacteria. *Journal of General Microbiology*, 1979, Vol. 111, 1, p 63-71. ISSN. 0022-1287
- 31) CORDES, Thorben et al. Wavelength and solvent independent photochemistry: the electrocyclic ring-closure of indolylfulgides. *Photochemical*. 2009, 8, 4, p. 528-534. ISSN 1474-905x. DOI: 10.1039/b817627b. Available online:
<http://xlink.rsc.org/?DOI=b817627b>

9. Attachments

9.1. MALDI-TOF MS Spectrum of unpurified 414 nm compound



Yellow: MS³ spectrum: 383 & 355 Orbitrap



9.2. ^1H NMR Spectrum of 9th minute fraction from C30-HPLC

